Thesis for the degree of Doctor of Philosophy

Design of Thermal Energy Storage with Phase Change Materials

Investigations within Material, Device and System Scale

Pepe Tan

Department of Architecture and Civil Engineering
Division of Building Technology
CHALMERS UNIVERSITY OF TECHNOLOGY
Göteborg, Sweden 2020

Design of Thermal Energy Storage with Phase Change Materials
Investigations within Material, Device and System Scale
Pepe Tan
ISBN 978-91-7905-304-8

Doktorsavhandlingar vid Chalmers tekniska högskola
Ny serie nr 4771
ISSN 0346-718X

Department of Architecture and Civil Engineering
Division of Building Technology
Chalmers University of Technology
SE–412 96 Göteborg, Sweden
Telephone + 46 (0) 31 – 772 1000

Typeset by the author using LaTeX.

Printed by Chalmers Reproservice
Göteborg, Sweden 2020

Everything has three sides
the one I see,
the one you see,
and the one nobody of us yet sees.
(A quote from an unknown source)

Abstract

The addition of a thermal energy storage (TES) into a process allows the operator to store and release thermal energy on demand. This increased process flexibility leads to potential benefits such as shifting energy demand from peak to off-peak hours. In particular, so called phase change materials (PCMs) have the potential to achieve high storage densities, when their latent heat of melting and solidification can be utilized. However, despite a high research interest in PCMs over the last years, real life implementations of PCM TES are still uncommon. This thesis presents work done on material, device and system scale based on a case study for daily peak shaving of cold energy in an office building using a PCM TES.

On material scale, the T-History method for thermal analysis of PCM samples has been studied with both numerical and experimental methods. It is shown that the current mathematical model is subject to systematic errors which should be corrected in the future. Moreover, the results of the method are shown to be sensitive to a number of different experimental parameters and their trade-offs are discussed. A new data evaluation method, which is more robust to noisy data when forming the first time derivative of the temperature measurements, is proposed in order to achieve a better trade-off between precision and accuracy of the results. The work can be seen as a contribution to the necessary standardization of the method in future work.

On device scale, an experimental test setup has been built to study a commercially available PCM TES design with a salt-hydrate as storage material. The test setup is used to cycle the storage under actual process conditions. The results show that the storage suffered from phase separation of the PCM with continued cycling, which causes the storage capacity to decrease. Sample analysis using the T-History method reveals that supercooling behavior, phase change temperature and storage capacity systematically changes across the vertical height of the storage before and after cycling. While it is shown that the phase separation can be reset, phase separation needs to be prevented when the storage is scaled up.

A techno-economic analysis on system scale is then performed for an actual real-scale installation of the PCM TES in a new office building. First benchmarking shows that the storage capacity is stable but does not reach manufacturer specifications. Future work needs to determine the reasons behind the performance decrease, such as looking into the role of a superabsorbent polymer that has been mixed with the salt-hydrate to prevent phase separation. The PCM TES can nevertheless be used for daily peak shaving. A mixed integer linear programming (MILP) model is used to optimize the storage discharging schedule for a simulated yearly cooling load of the building. The estimated economic benefits are translated into an investment cost limit for a five year payback time. Since the current storage investment costs are significantly higher than this limit, future work should prioritize finding the boundaries of economic feasible storage applications.

Keywords: Phase Change Materials, Thermal Energy Storage, T-History, Experimentation, MILP

Acknowledgments

This PhD thesis marks the end of a journey that started five years ago and I would like to use this page to leave a few formal and personal notes. The project was made possible through funding from the Swedish Energy Agency (Energimyndigheten), the Swedish Centre for Innovation and Quality in the Built Environment (IQ Samhällsbyggnad), Chalmers Energy Area of Advance and the Swedish Environmental Protection Agency (Naturvårdsverket). It also received financial support from the EU project IRIS Smart Cities and the FED - fossil free energy districs project. Their funding is gratefully acknowledged.

Moreover, I would like to express my gratitude to Angela Sasic Kalagasidis and Pär Johansson for taking me in as their PhD student and for their supervision during these years. Their ideas and continuous support helped shaping this work considerably. The publications listed in this thesis wouldn't have been possible without their advice and detailed comments on every initial manuscript. Thank you also for giving me the experience of teaching within your courses. Next, I would like to thank Per Löveryd (Akademiska Hus AB), Patrik Lindberg (ÅF Pöyry AB), Kaia Eichler (ÅF Pöyry AB) and Urban Kalin (LG Contracting AB), who made the case study in this thesis a reality. Thanks also go to the thermal analysis group of ZAE Bayern in Wuerzburg, who hosted me during a study visit.

A special thank you go to Josef, Kaj, Fredrik and Quan for the shared time over these years. I will miss all the interesting conversations across our desks or over lunch & coffee. Thank you also to my former colleagues Roland and Raheb for your nice company as roommates when we were still in much smaller offices. I am also grateful to Ingela, Marek and Tommie for their help with administration and in the laboratory.

Lastly, thank you to my family for always supporting me. And thank you, Maomao, for simply being such a wonderful person.

It is overwhelming to see how severely the world has been changed in these last months by the new Coronavirus and I can only wish that the loss of lives and suffering ends as soon as possible. It gives me solace and hope knowing that medical sciences has never been as advanced as it is now to quickly find effective treatments. Until then, please stay safe and healthy.

Pepe Tan
Göteborg, May 2020

List of Publications

This thesis is based on the following four appended papers:

First Theme: Calorimetry of PCMs using the T-History method

Paper 1. Pepe Tan, Michael Brütting, Stephan Vidi, Hans-Peter Ebert, Pär Johansson, Helén Jansson, Angela Sasic Kalagasidis. *Correction of the enthalpy–temperature curve of phase change materials obtained from the T-History method based on a transient heat conduction model.* International Journal of Heat and Mass Transfer, Vol. 105, p. 573-588, 2017.

Paper 2. Pepe Tan, Michael Brütting, Stephan Vidi, Hans-Peter Ebert, Pär Johansson, Angela Sasic Kalagasidis. *Characterizing phase change materials using the T-History method: On the factors influencing the accuracy and precision of the enthalpy-temperature curve.* Thermochimica Acta, Vol. 666, p. 212-228, 2018.

Second Theme: Laboratory scale analysis of a PCM TES

Paper 3. Pepe Tan, Patrik Lindberg, Kaia Eichler, Per Löveryd, Pär Johansson, Angela Sasic Kalagasidis. *Effect of phase separation and supercooling on the storage capacity in a commercial latent heat thermal energy storage: Experimental cycling of a salt hydrate PCM.* Journal of Energy Storage, Vol. 29, Article No. 101266, 2020.

Third Theme: System scale analysis of a PCM TES

Paper 4. Pepe Tan, Patrik Lindberg, Kaia Eichler, Per Löveryd, Pär Johansson, Angela Sasic Kalagasidis. *Thermal energy storage using PCMs: Techno-economic evaluation of a cold storage Installation in an office building.* (Submitted to Applied Energy on 24th Feb. 2020, currently under review).

Paper 1 investigates the T-History method for measuring the enthalpy over temperature curve of small PCM samples. Based on a numerical study it is shown that the current underlying mathematical model causes a systematic overestimation of the sensible specific heat capacities and an underestimation of the latent heat, if the insulation thermal mass is neglected.

Paper 2 contains a study of different experimental setups for the T-History method. Relevant factors influencing the measurement accuracy and precision are discussed. It is shown that the first derivative of the temperature over time data should be carefully cleared from noise in order to avoid over- or underestimation of the latent heat. Moreover, the latter is systematically underestimated when a smaller sample mass compared to the sample holder and insulation is used. This result supports the conclusion made in paper 1.

Paper 3 contains an experimental study of a commercial PCM TES design using a commercially available salt-hydrate PCM. The PCM TES is evaluated using a laboratory setup consisting of about 125 L PCM. It is shown that the effect of phase separation and supercooling decreases the storage capacity considerably after only a few cycles. In the paper, possible reasons for this capacity decrease are discussed and compared with T-History measurements.

Paper 4 analyzes the PCM TES from the third paper as a full scale installation with 7000 L PCM. The PCM has been modified by the storage supplier with an additive to prevent the previously observed phase separation. The storage is operated for daily peak shaving in an office building. Charging and discharging measurements are presented. The storage is modeled numerically and an economic investigation is performed based on a scheduling optimization model.

The thesis is a continuation of a previous licentiate thesis:

Pepe Tan. *On the design considerations for thermal energy storage with phase change materials: Material characterization and modelling.* Licentiate Thesis. Chalmers University of Technology. 2018. Available online: `https://research.chalmers.se/publication/500367`

List of Symbols

List of Abbreviations

amb	Ambient
ch	Charging
dch	Discharging
ref	Reference material
t,tube	Sample holder tube
L	Liquid phase
S	Solid phase
EXT	Exterior
HEX	Heat exchanger
HTF	Heat transfer fluid
INS	Insulation
INT	Interior
PCM	Phase change material
SAP	Superabsorbent polymer
TES	Thermal energy storage
WALL	Wall between phase change material and heat transfer fluid

List of Greek Symbols

δ	Storage density ($\mathrm{J\,m^{-3}}$)
η	Efficiency/Effectiveness (-)
θ	Ratio of storage capacities (-)
λ	Thermal conductivity ($\mathrm{W\,m^{-1}\,K^{-1}}$)

ρ	Density ($\mathrm{kg\,m^{-3}}$)

List of Roman Symbols

A	Area ($\mathrm{m^2}$)
c_p	Specific heat capacity ($\mathrm{J\,kg^{-1}\,K^{-1}}$)
d	Distance or diameter (m)
e	T-History correction factor for heat flux (-)
H	Enthalpy (J)
h	Specific (mass or volume) enthalpy ($\mathrm{J\,kg^{-1}}$ or $\mathrm{J\,m^{-3}}$)
L	Latent heat of melting and solidification ($\mathrm{J\,kg^{-1}}$) or length (m)
m	Mass (kg)
$\dot{m}$	Mass flow rate ($\mathrm{kg\,s^{-1}}$)
P	Power (W)
Q	Storage capacity (J)
$\dot{Q}$	Heat flux (W)
$\dot{q}$	Heat flux density ($\mathrm{W\,m^{-2}}$)
r	Radius (m)
R_{th}	Thermal resistance ($\mathrm{K\,W^{-1}}$)
T	Temperature (°C)
t	Time (s)
U	Internal Energy (J)
u	Velocity ($\mathrm{m\,s^{-1}}$)
V	Volume ($\mathrm{m^3}$)
$\dot{V}$	Volumetric flow rate ($\mathrm{m^3\,s^{-1}}$)

List of Figures

List of Tables

Contents

Part I

Summary

Chapter 1

Introduction

1.1 Thermal energy storage with phase change materials

The current energy landscape continues to transform towards more flexibility on both the supply and demand side [1]. In building applications for example, heating and cooling energy demands vary on different temporal scales depending on the local climate and occupancy. On the supply side, the shift from traditional centralized fossil fuels to decentralized renewable energies add an increased mismatch between availability and demand of different energy sources in the system. Within this context, the installation of a thermal energy storage (TES) into a process allows the process operator to move heat or cold energy across time by charging and discharging the storage on demand [2–5]. This is especially beneficial when, for example, differences in energy prices can be utilized [6–9].

Table 1.1: Overview of different TES concepts given by [10].

Concept	Storage parameter	Technology level	Example
Sensible heat	$c_p \cdot \Delta T$ in $\mathrm{J\,kg^{-1}}$	Commercially available	Hot/cold water tank, rock bed storage
Latent heat	L, $c_p \cdot \Delta T$ in $\mathrm{J\,kg^{-1}}$	Demonstration projects to commercially available (mostly ice storage)	Solid to liquid transition of PCMs (see Tab. 1.2)
Thermochemical	Heat of reaction/sorption	R&D to demonstration projects	Metal sulphate reaction systems, Silica gel/water & Zeolite/water sorption systems

Tab. 1.1 lists possible concepts of storing thermal energy. Among them, the utilization of the latent heat of solidification and melting has been discussed for TES applications (Fig. 1.1) [11–16]. When the latent heat of the storage material can be utilized (L in $\mathrm{J\,kg^{-1}}$), significantly higher storage densities are theoretically possible

(Fig. 1.2). This concept is not new, as ice storages have been successfully installed in order to benefit from varying daily electricity prices since the 1980s [5, 17]. However, in order to utilize latent heat storages in systems that work above the freezing point of water, considerable research attention has been given to so called phase change materials (PCMs). PCMs within a wide range of melting and solidification temperatures and different building applications have been discussed in the literature [12, 18–22]. PCMs that are commercially available within the temperature range of building applications are typically paraffins or salt-hydrates (see Tab 1.2).

(a) Liquid state (b) Solid state

Figure 1.1: Phase change of two commercial PCMs (left sample holder: salt hydrate, right sample holder: paraffin)

Table 1.2: Typical properties of (commercially available) PCMs for building applications (Temperature range: −10..100 °C). More material classes and detailed classifications can be found in [11–13, 16, 21, 23–25].

	ρ in $\mathrm{kg\,m^{-3}}$	c_p in $\mathrm{J\,kg^{-1}\,K^{-1}}$	L in $\mathrm{kJ\,kg^{-1}}$	λ in $\mathrm{W\,m^{-1}\,K^{-1}}$
Water	1000	4180	330	0.6
Paraffins	ca. 700-900	ca. 2000	ca. 150-250	ca. 0.2
Salt-Hydrates	ca. 1300-1500	ca. 3-4000	ca. 150-250	ca. 0.4-0.6

The benefit of high heat storage densities using PCMs is only achieved when the latent heat of the storage material can act on its own, i.e. as a matching heat source or sink with respect to the temperature levels of the process as shown in Fig. 1.3 and with sufficient time for heat exchange. However, designing a PCM TES is currently still an active field of research and no general guidelines exist. There is therefore a need to define and study the design task in a more systematic way.

In the next sections, the necessary steps for designing a PCM TES are outlined in more detail. Research needs at certain stages are discussed based on an overview of the current PCM TES literature. Moreover, the scope and limitations of the thesis are presented based on a case study for a cold storage application in an office building.

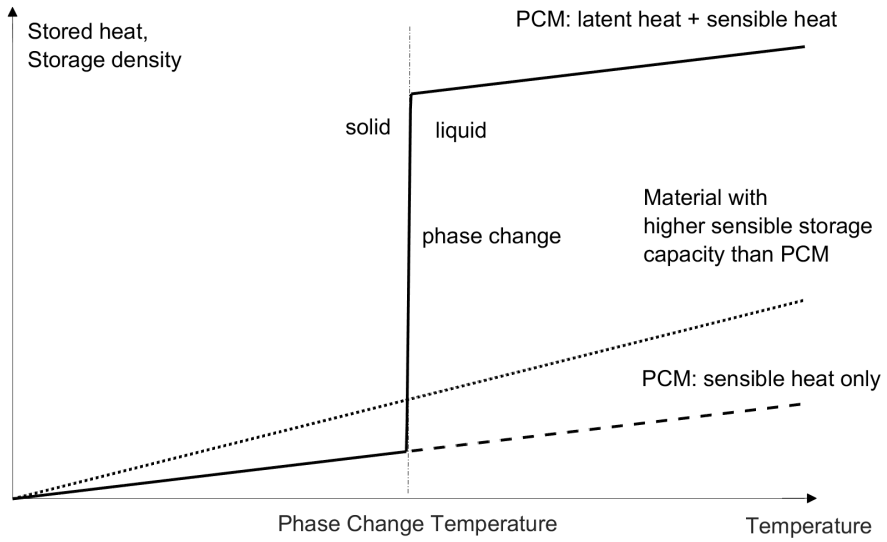

Figure 1.2: Illustration of the storage potential of a (solid-liquid) phase change.

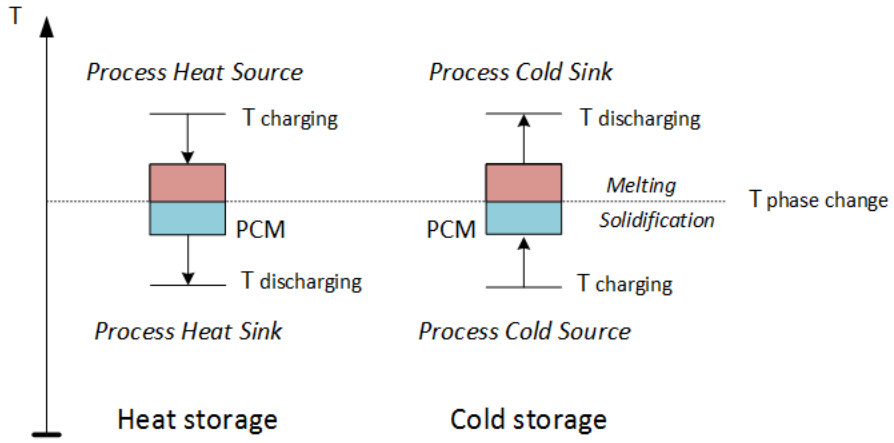

Figure 1.3: Illustration of the process temperature levels for (dis)charging a PCM TES depending on a heat or cold storage application. Due to irreversibility of the (dis)charging processes, any heat and cold storage will supply the process heat/cold sink at a lower (heat storage) or higher (cold storage) temperature, respectively (compared to the original process heat/cold source). Constraints on the available (dis)charge time from the process also have to be considered.

1.2 Literature overview

During the 1970s, PCMs as storage material received first attention together with the interest in renewable energy due to the oil crisis. A broad overview of the conducted research from this era is summarized by Lane [26, 27]. The conclusion was that a few commercially available small scale PCM TES were developed and sold. However, the majority of attempts were not economically feasible due to instable material properties and high costs. After the oil crisis, the interest in PCM TES has remained at a relatively constant level. This changed again from the 2000s onwards, when

research in PCM has seen a significant surge as shown in Fig. 1.4[1]. Review articles from this period show that these numbers reflect the possible combinations between a large amount of considered materials and a wide range of new potential applications [11–16].

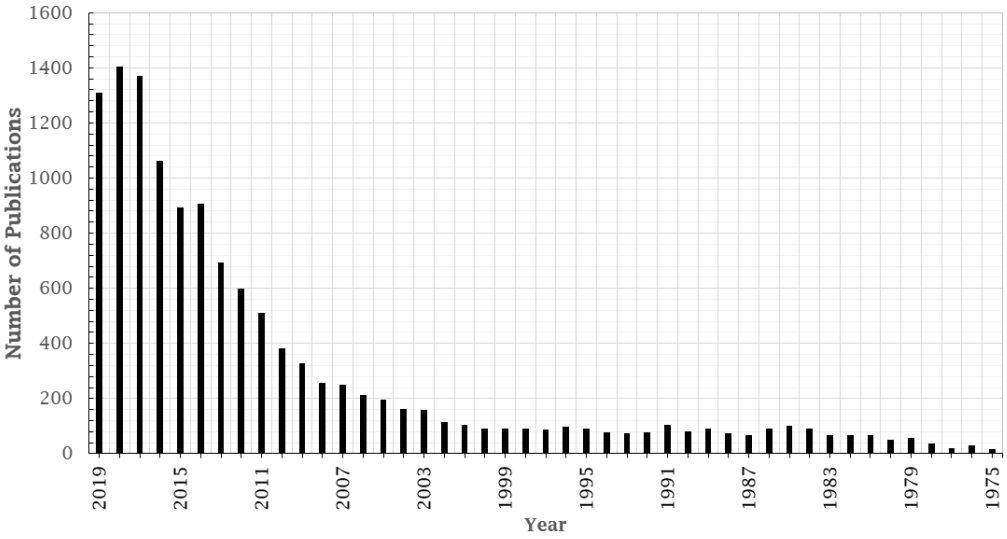

Figure 1.4: Number of Scopus indexed publications related to PCM TES in general (from September 2019)

In the following, the discussion is limited to so called actively controlled PCM TES applications [28]. In such an application, the process operator determines when heat/cold energy should be transferred into (charging) or from (discharging) the storage material. Transfer of thermal energy between the process and storage occurs via the process heat transfer fluid (HTF) that consists typically of air or water for building applications [29]. The storage can then be seen as a heat exchanger that moves thermal energy across time between the process heat sources and sinks.

It is notable that despite the potential benefits mentioned in section 1.1, currently very few of such active PCM TES have been integrated in existing processes [5, 16]. Available commercial PCM products typically are used for small scale and/or passive applications such as cold transportation boxes, textiles or wallboards [14, 16]. In these passive applications, the latent heat of PCM is included with the design intent to achieve a higher thermal mass and stable temperatures [4, 30–32].

Since a very low number of commercial products are available and little experience with actual PCM TES installations have been reported, the design of a PCM TES and the development of general design guidelines is a developing field of research.

Integrating a PCM TES into a system can be grouped into a series of logical steps done on material, device and system scale as shown in the flowchart of Fig.

[1]Fig. 1.4 is generated using Scopus entries that contained all of the words: 'Phase' 'Change' 'Material' 'Energy' 'Storage' or 'Latent' 'Heat' 'Energy' 'Storage' in either title, abstract or keywords. Publications with the terms 'battery' and 'batteries' were filtered out from the results.

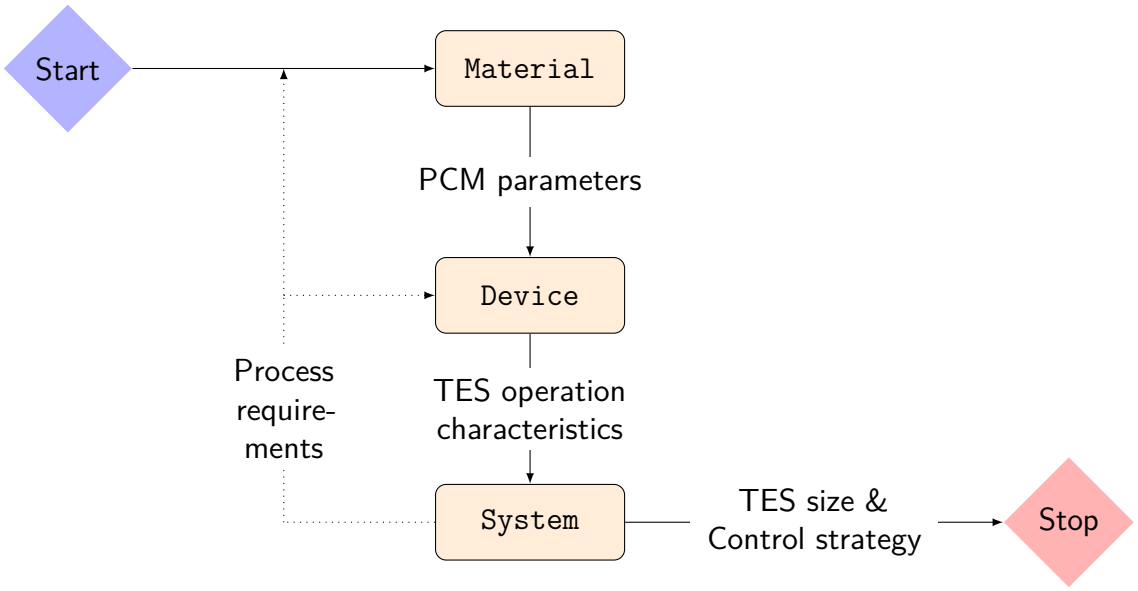

Figure 1.5: Illustrative flowchart of design steps for a PCM TES

1.5. The different scales are interconnected as they each provide input parameters to their respective next scale:

1. **Material scale:** Characterization and selection of a suitable PCM based on process requirements.

   The PCM with its phase change temperature needs to be chosen so that melting and solidification can occur within the available process temperature boundaries. A high latent heat is desirable in order to achieve an increased theoretical possible storage density (compared to sensible storage materials) and low specific storage costs. Further minimum requirements for PCMs are stability with consecutive melting and solidification cycles, non-corrosiveness as well as low health and safety risks (e.g. with respect to toxicity and flammability). It is moreover desirable that the PCM features a high thermal conductivity and low degree of volume change for an easier application on device scale.

2. **Device scale:** Design of heat exchange between PCM and HTF of the PCM TES based on process requirements.

   The goal in this step is to design the storage so that as much as possible of the theoretical storage capacity of the PCM can be utilized within the process. Moreover, the desired power during storage charging and discharging should be achieved, so that the installed storage capacity can be utilized within available time limits. The available temperature difference between process HTF and phase change temperature, the material thermal conductivities and the HTF flow rate determine the necessary heat transfer area for reaching a certain discharge or charging power and capacity of the storage.

   In the literature, two basic configuration principles for heat exchange are common: The PCM is either macro-encapsulated into several separate containers

or located in bulk surrounding the heat exchanger. In the former case, the macro-encapsulated PCM can be arranged either into a packed bed or arranged into a heat exchanger geometry with regular flow channels for the HTF. For the latter case, the PCM TES resembles a shell and tube heat exchanger similar to common ice storages. Macro-encapsulated PCM have been mostly studied in free-cooling applications using air as HTF, while a liquid HTF is typically used for shell and tube heat exchangers.

3. **System scale:** Optimization of TES size and control strategy within the process

   The performance of the PCM TES device during charging and discharging has to be evaluated regarding its achievable process benefits on system level. Here, a control strategy needs to be defined so that economic and/or ecological benefits of the storage to the process operator are fully utilized. This is an optimization task that typically takes into consideration the storage size, availability of process sources and sinks as well as their energy prices. When taking into account the storage investment costs, an economic analysis of different possible alternatives of the device scale should also be performed.

Table 1.3 presents a literature overview that are grouped into the above scales. It can be summarized that PCM TES research has a number of key challenges.

On material scale, a variety of potential PCMs have been listed based on their latent heat and phase change temperature across a wide temperature range [11–16]. However, trade-offs exist among different material classes. Organic materials, such as paraffins, are less corrosive and more stable compared to inorganic PCMs. But on the other hand, they may be more expensive and have an additional safety risk due to their flammability [33]. Salt-Hydrates in turn are considerably cheaper (up to four times, see section 1.3) but have to be studied regarding their cycling stability [26, 27, 34–37] and corrosion [38–41]. A major research area is that measurement methods, which determine important material properties such as phase change temperature, storage capacity, thermal conductivity as well as thermal stability, are not standardized [42–46]. Therefore, there is research required to obtain accurate material properties in order to predict the actual material performance in the storage.

On device scale, extensive experimental and numerical work has been already done to model and improve heat exchange between PCM and HTF in various heat exchanger geometries [47–50]. However, in order to establish general guidelines or models, further research is needed to study their applicability on full-scale storages. It was also pointed out that the idealization of material properties in the numerical models should be always compared against experiments and not extrapolated outside of their validity [47]. A difficulty here is that these models require input parameters from material scale measurements. However, these can yield varying results for the same PCM due to the lack of standardized testing [48]. A further limitation is that these guidelines are usually not evaluated based on process requirements [49]. Moreover, an economic and life cycle cost analysis of the various proposed storage devices is rarely performed [47, 51–53]. It is however necessary to evaluate

the technical performance of a PCM TES based on its costs in order to compare it to existing storage technologies such as sensible storages.

On system scale, the low number of existing PCM TES installations and commercial products are a contrast to the large amount of research done on device and material scale [29, 54, 55]. On this scale, work has focused to optimize storage control using different methodologies [6–9, 56]. These works were applied mostly on ice storages, since they are more commonly installed. Here, the objective is usually to maximize the economic and/or ecological benefits of the storage within the process. It should be noted that the few existing works, which focus on system optimization of a PCM TES also typically use an idealized PCM model [57, 58]. Considering the research needed on material and device scale, more aspects may have to be considered when the storage is scaled up in reality.

It can be seen from the literature overview that many important topics on PCMs have been already studied. However, these aspects are usually scattered and presented in an isolated way. This can be seen as a limiting factor for successful PCM TES applications to emerge from the research. An example would be to focus on improving technical PCM TES parameters on device scale, such as increasing the heat transfer rates, but not analyzing the cost to benefit ratio of these improvements for the process on system scale. For a good design however, a more holistic view on all these aspects would be necessary.

Methodologies and design tools are thus necessary that enable a decision making process when designing a PCM TES. Recent working groups among researchers have started to address this research gap. For example, the IEA ECES Annexes 30 and 31 [59–61] proposed to define common key performance indicators (KPI) for thermal energy storage technologies. This allows a systematic comparison of different TES designs and technologies within a given process. However, a common limitation here is that economic key performance indicators are usually not reported [61].

The work presented in this thesis aims to contribute in the areas of material characterization and towards a more techno-economic view of the design process. It presents work on material, device and system scale for designing a PCM TES based on a single yet comprehensive and fully documented case study.

Table 1.3: Overview of representative articles on different scales. When available, review articles are listed as references in this table. Text in *italics* are additional remarks made by the author of this thesis.

Scale	Topic	Reference	Content	Challenges
Material	Overview of available PCMs	[11–16]	Information about phase change temperature and latent heat for different material classes.	Commercial success more common in (small-scale) passive applications than active storage systems. More need for low-cost and technically reliable PCMs.
	Measurement methods	[42–46]	A range of conventional and non-conventional methods are available. Major focus is on determining latent heat and phase change temperature	Measurement standardization for all material properties during phase change is needed.
	Corrosion	[38–41]	Results on corrosion of metals by salt-hydrates	*Difficult to compare the findings due to lack of test standards.*
	Thermal stability	[26, 27, 34–37]	Inorganic PCMs show more cycling degradation compared to organic PCMs	Test standard is needed.
	Safety and health hazards	[33]	Available PCMs have varying degrees of toxicity to the human body. Possible eye/skin irritation with contact is common.	Lack of fire safety and retardation studies for flammable PCMs.
	Volume change	[62]	Only organic PCMs studied; Volume change from negligible up to 23.53 % possible	Studies on volume change for other materials than organic PCMs needed.
	Proposal of new/modified PCMs	[63–67]	Strong focus on enhancement of thermal conductivity. Modification using additives or micro-encapsulation	*Cost/benefit ratio of enhancements is usually not reported.*
	Material costs	[68]	Salt-Hydrates are commonly commercially available	Material databases with standardized testing needed. *Material costs alone may not reflect actual storage costs.*
Device	Modeling of PCM TES	[47, 48]	Overview of numerical models for phase change and for different TES geometries	More validation needed of idealized PCM models. Lack of economic analysis.
	Heat transfer design	[49, 50, 69]	Overview of empirical and numerical methodologies to predict heat transfer correlations in various geometries. Derivation based on laboratory setups	Applicability may be limited to their respective boundary conditions. *Scalability to full scale setup should be tested*
	Heat transfer enhancement	[51]	Overview of suggestions about increasing heat transfer area and/or thermal conductivities	Lack of cost/benefit ratio analysis.
	Macro-encapsulation	[52, 53]	Risk of PCM leakage has been reported.	*Lack of economic and life cycle cost analysis.*
System	Overview of proposed PCM TES applications	[29, 54, 55]	Focus mostly on technical feasibility	Economic analysis and comparison to storage alternatives needed.
	Optimum TES control	[6–9, 56]	Different optimization methodologies available	Optimized control models mostly for ice or sensible TES. Reported control strategies for PCM TES applications focus on free-cooling applications and follow simple rule-based control.
	Optimum TES sizing	[57, 58]	Optimization of LCC costs	*Use of idealized PCM TES model.*

1.3 Case study: PCM cold storage for peak shaving applications

The case study was done in collaboration with Akademiska Hus and ÅF Pöyry AB. It involved integrating a commercial PCM TES for storing cold thermal energy for an office building [70]. In the following sections, the process boundaries and the selection process for the PCM TES are summarized.

1.3.1 Process description

The office building has been constructed on Chalmers University of Technology Campus Johanneberg in 2019. The building is connected to the campus district cooling system in order to provide comfort cooling to the office spaces via an air handling unit (AHU). Water is used as HTF in this application. In the original process, the AHU is supplied with cold energy only from district cooling to cover the building cooling demand. However, cooling load simulations of the building showed that the additional cooling demand (up to 402 kW) will contribute significantly to an increased peak cooling load of the district cooling system for critical days.

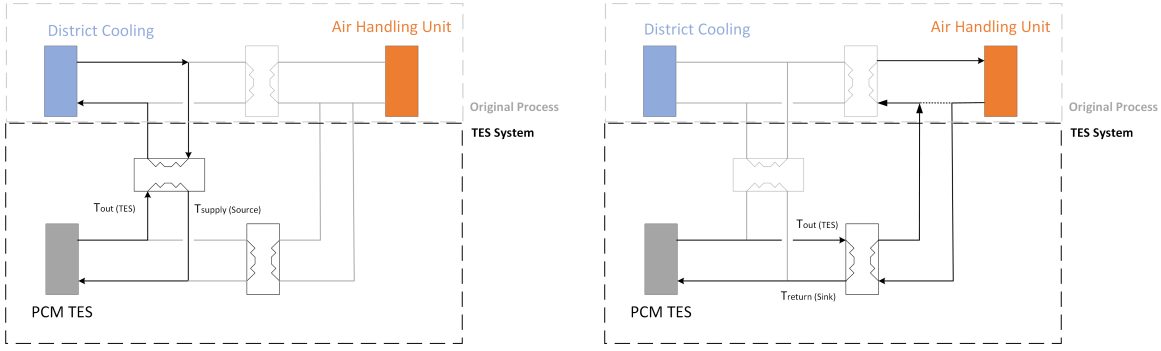

(a) TES charging (b) TES discharging

Figure 1.6: TES integration for a AHU cooling process.

Therefore, it was seen as beneficial to add a PCM TES for storing cold energy into the building system as shown in Fig. 1.6 as it allows a reduction of the peak cold energy load for the district cooling system within a small storage volume. The PCM TES is intended to be operated as daily storage. It is to be charged during night using the campus district cooling system and discharged during the day, when there is usually a high building cooling load. Moreover, the process owner benefits from differences in energy prices between high and low cooling load scenarios based on the local energy tariff.

Table 1.4 shows the temperature boundaries of the process source and sink for charging and discharging the storage. The TES is considered as fully charged at $T = T_{supply}^{Source}$ and fully discharged at $T = T_{return}^{Sink}$. The maximum temperature difference for the TES is then $\Delta T_{max} \approx 8 - 10°C$.

Table 1.4: Temperatures for the AHU process

	Value	Comment
$T_{supply}^{Source} = T_{charging}$	8 °C	Constant temperature supplied by the cooling system to the TES inlet during charging.
$T_{return}^{Sink} = T_{discharging}$	16-18 °C	Constant return temperature of the AHU at the TES inlet during discharging.
T_{cutoff}	14 °C	Maximum acceptable temperature by the AHU at the TES outlet during discharging.

During discharging, a cutoff condition is given for the storage outlet temperature as $T_{out} < T_{cutoff} = 14°C$, since a temperature higher than this limit is not considered to be useful to reduce the AHU cooling load.

For a specified known mass flow rate $\dot{m}_{HTF}$, the achievable (dis-)charging power output of the TES is directly given by the HTF temperature difference between inlet and outlet:

$$P_{TES}^{ch}(t) = \dot{m}_{HTF}^{ch} \cdot c_{p,HTF}(T_{supply}^{Source} - T_{out}(t)) \tag{1.1a}$$

$$P_{TES}^{dch}(t) = \dot{m}_{HTF}^{dch} \cdot c_{p,HTF}(T_{return}^{Sink} - T_{out}(t)) \tag{1.1b}$$

The (dis-)charged capacity of the TES over time is then:

$$Q_{TES}(t) = \int_0^t P_{TES}(t)\mathrm{d}t \tag{1.2}$$

1.3.2 Selection of PCM TES supplier

A number of options were considered in order to find a suitable PCM TES for the case study. The complete process is summarized in an internal report [70] and outlined in this section. Since the latent heat of a PCM is to be used as storage material, it has to have a melting temperature within the temperature interval of $T_{supply}^{Source} = 8°C < T_{PCM} < T_{cutoff} = 14°C$ in order to be feasible for the process. This requirement was ruled out by most of the contacted PCM suppliers, as they did not offer PCMs for this narrow temperature range. Moreover, due to the generally high costs of PCMs, only commercial salt-hydrates were found to be feasible within the available budget. In the end, two PCMs and storage designs from two different suppliers remained as options for the application.

The first design featured macro-encapsulated rectangular PCM containers, which were stacked inside a cylindrical storage tank. Its working principle follows a packed bed heat exchanger as the heat transfer fluid (HTF) is intended to flow through the gaps in the stacked container bed. The design was already investigated in previous works by Jokiel (2016) [71] and Alam et al. (2019) [72]. This option was not chosen in the project as there was a risk of PCM leakages from the macro-encapsulation that would contaminate the HTF. It was concluded that detecting a PCM leakage would be difficult in practice. As salt-hydrates are corrosive to metal [39, 41], long-term

stability of the piping and measurement equipment in contact with the HTF had to be guaranteed.

The chosen design was a commercially available storage tank filled with PCM as bulk material that has not been described in the literature before. The complete storage is sold by Rubitherm GmbH [73], which also produces the PCM. The company BEKA Heiz- und Kühlmatten GmbH [74] is the supplier of the heat exchanger parts of the storage. The HTF flows through a dense arrangement of plastic heat exchanger tubes similar to a shell and tube heat exchanger. The heat exchanger design is also available for ice storages [74]. This design was seen to have a lower PCM leakage risk compared to the first alternative. In case of a leakage from the heat exchanger tubes, HTF would flow inside the storage container and cause the interior volume to expand. Such an event is easier to detect and the operation of the storage can be stopped. Moreover, the supplier was able to deliver both the PCM and storage within the available project time frame and budget. The PCM is a commercial salt-hydrate (SP11) with a relatively low material price of 3.53 EUR/kg [2]. Furthermore, it showed acceptable low health and fire hazards according to the safety data sheet [75]. A paraffin (RT10HC) from the same supplier was also found to be potentially suitable [76]. However, this PCM was not further considered as its price was over four times higher compared to SP11 (14.94 EUR/kg). Since the heat exchanger is corrosion resistant against the salt-hydrate, a low thermal conductivity of the heat exchanger material is accepted as trade-off. As a consequence, flow rates of the HTF are within the laminar flow regime (Reynolds number <100) in order to match the low heat transfer rates between the HTF and PCM. An overview of the trade-offs with respect to the chosen PCM and heat exchanger materials is given in Tab. 1.5.

For this thesis, two storages were purchased and studied. A small scale laboratory prototype and a full-scale installation. A detailed description of each of the storages is given in the later chapters of this thesis.

Table 1.5: Summary of PCM TES choice.

	Benefits	Drawbacks / Risks
PCM: SP11	Significantly lower price than paraffin Relatively high storage density Relatively high thermal conductivity Lower flammability then paraffin Availability within project time frame	Corrosive to metals Risk of supercooling Risk of phase separation Risk of incongruent phase transition Unknown chemical composition
Heat Exchanger	More robust to leakage compared to macro-encapsulation Non-corrosive to SP11 Scalability Same supplier as PCM material Availability within project time frame	Low thermal conductivity of tube material Laminar HTF flow

[2] or 37.59 SEK/kg with a conversion rate of 10.65 SEK/EUR

1.4 Thesis outline

The presented case study is used to follow the PCM TES design process from material to system scale. The chapters 2-4 present a summary of the work done in order to improve this design process. Each chapter begins with a more detailed overview of the research background and motivation of the work within each design scale. At the end of a chapter, conclusions of the work are given together with a recommendation for future research.

Chapter 2 aims towards the improvement and standardization of the so called T-History method to measure the phase change temperature and storage capacity of PCMs on samples in the range of several grams. The chapter is a summary of **Paper 1** and **Paper 2**. It discusses parameters influencing the accuracy and precision of the method using a numerical and experimental approach. This work was done together with the Bavarian Center for Applied Energy Research e.V. (ZAE Bayern) and can be used to measure PCMs for different applications.

Chapter 3 presents the experimental results from a laboratory storage, which is a downsized copy of the full scale PCM TES from the case study of section 1.3. A test setup and methodology is developed in order to predict the achievable storage capacity and storage density within the given process parameters of the case study. The work evaluates the risks of using the commercial salt-hydrate in the storage device due to the material instabilities listed in Tab. 1.5. Chapter 3 is a summary of **Paper 3**.

Chapter 4 presents experimental and numerical results from **Paper 4**, in which the full scale PCM TES has been analyzed on system scale. It discusses the measured power and storage capacity within the actual process and provides an estimate on the achievable economic benefits of the current design and alternative options.

Chapter 5 and 6 summarize the findings into general conclusions for the design process of a PCM TES and recommendations for future work, respectively.

1.5 Limitations

Methodologies and decision tools always have inherent limitations that are based on both a limited scope and simplifications that influence the accuracy of the results (see Fig. 1.7).

On material scale, the reliability of choosing a PCM based on its material properties is limited by the accuracy of the measurement method itself. It was shown in **Paper 1** and **Paper 2** that the T-History method is still subject to systematic measurement errors, which have to be corrected in the future. In this work, only the latent heat and phase change temperature was characterized. Other relevant material properties such as density and thermal conductivity are based on available values from the manufacturer and have not been measured rigorously.

On device and system level, only the given design of the PCM manufacturer is experimentally studied in **Paper 3** and **Paper 4**. Due to the instable material performance, modeling of the storage and improvements of the heat exchanger geometry was not attempted in detail. A major limitation in **Paper 4** were inconsistent

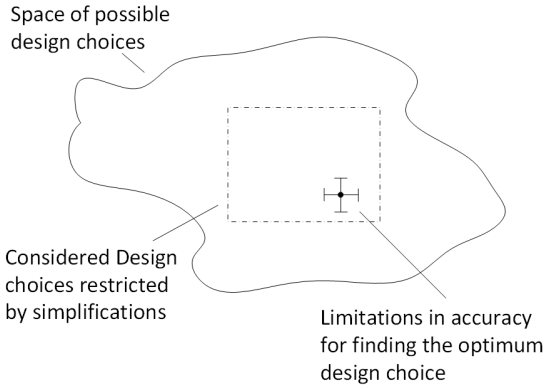

Figure 1.7: Illustration of the limitations

results from the internal temperature sensors of the full-scale tank. The exact reasons behind the measured tank performance is at the time of this thesis still unknown and a better understanding of the tank performance has to be determined together with the storage manufacturer. The numerical model describing the PCM TES is thus necessarily speculative and may need to be revised in future work.

While reproducibility and repeatability of the results was a focus, the presented number of measurements may not reflect the multi-year performance of the storage. Moreover, the study in **Paper 4** is only done within the building system. However, the impact of operating the PCM TES on the district cooling plants should be evaluated as well. The case study should be extended with other TES options, most notably sensible storages in order to place the PCM TES performance into perspective with reference technologies. Furthermore, ecological factors have not been studied in this work. It is clear that these are also important, considering that utilizing the storage is always associated with a loss of energy. Other not addressed aspects are the environmental impacts of production and decommissioning of the PCM TES.

Chapter 2

PCM characterization using the T-History method

2.1 Background and motivation

Obtaining accurate and representative material properties for PCMs can be seen as a key research area. This is because the accuracy of any numerical model depends on correct material properties as input parameters.

For TES materials, it is important to estimate the storage capacity within the temperature range of the given application. In general, a change in the state quantity enthalpy is defined to be equal to the heat stored or released when the pressure is assumed to be constant [12].

$$\mathrm{d}U = \mathrm{d}Q - p\mathrm{d}V \tag{2.1a}$$

$$\mathrm{d}H = \mathrm{d}U + p\mathrm{d}V + V\mathrm{d}p \tag{2.1b}$$

$$\mathrm{d}H = \mathrm{d}Q \quad \text{for} \quad \mathrm{d}p = 0 \tag{2.1c}$$

It is therefore useful to plot the enthalpy change over the relevant temperature range in order to evaluate the storage potential of any material to be used for a TES. The mass specific enthalpy h ($\mathrm{J\,kg^{-1}}$) can be expressed via the mass specific (isobaric) heat capacity c_p ($\mathrm{J\,K^{-1}\,kg^{-1}}$), latent heat L ($\mathrm{J\,kg^{-1}}$) and the temperature change of the material.

$$\Delta h_{1-2} = \int_{T_1}^{T_2} c_p(T)\ \mathrm{d}T + \int_{T_1}^{T_2} \frac{\mathrm{d}F(T)}{\mathrm{d}T} L\ \mathrm{d}T \tag{2.2}$$

Fig. 2.1 shows idealized enthalpy over temperature curves for two PCM cases. For a pure substance, melting/solidification happens sharply at its phase change temperature T_{PCM} and occurs at this constant temperature until the material completely melts or solidifies. The liquid and solid states are separated by its latent heat of melting and solidification L. For a mixture of at least two substances, a temperature range typically exists, which is defined by the material composition.

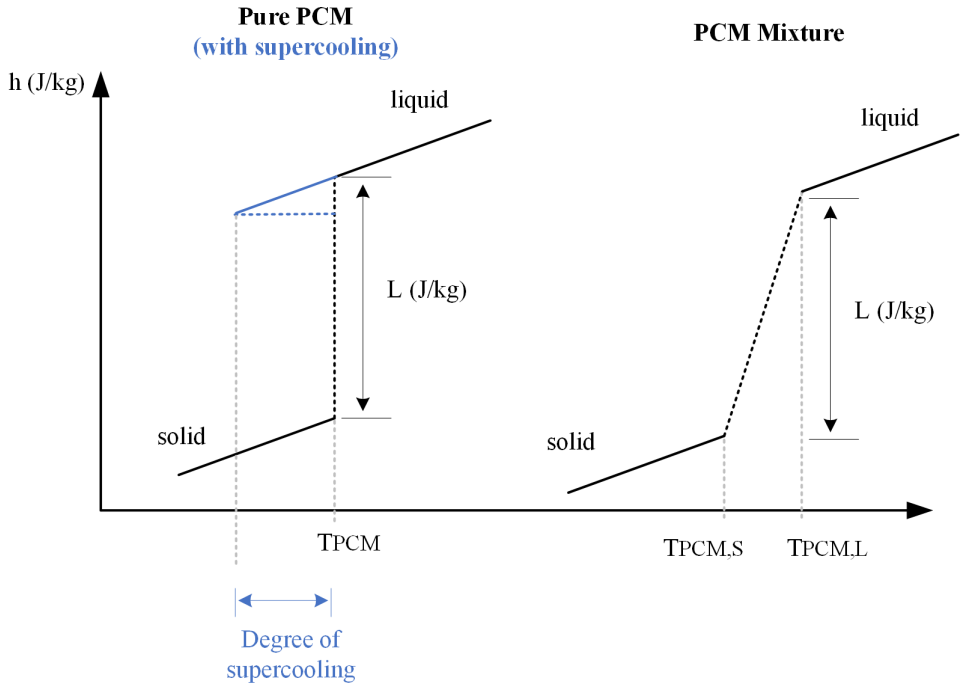

Figure 2.1: Schematic of enthalpy over temperature curve for pure and composite substances (redrawn from [46, 77]).

T^S_{PCM} and T^L_{PCM} are then the temperatures for when the mixture is completely solidified or melted, respectively. The enthalpy change between two temperature states can then be expressed via Eq. 2.2. In the equation, a temperature dependent function $F(T)$ describes the transition between solid and liquid states. When the exact composition of the PCM is known e.g. from a phase diagram, the phase change region can be reconstructed rigorously as shown in Gibout et al. [46]. If the composition is unknown, an approximation has to be made. For example by assuming a linear function for $F(T)$.

Available methods to derive the temperature dependent enthalpy curve are listed in Tab. 2.1. Traditional devices, such as differential scanning calorimeters (DSC), are typically designed to measure the specific heat capacity in only solid or liquid phase of a pure material and not explicitly for phase change [42]. In recent years, the use of these methods have been critically evaluated when measuring PCMs.

Latent and sensible heat are commonly lumped together using an effective (or apparent) heat capacity c_p^{eff}. When the sample undergoes melting or solidification, the instrument sees an apparent peak of the specific heat capacity at its phase change temperature. This is due to the additional storage or release of latent heat, respectively. In the evaluation of the data, it is commonly assumed that the sample is of uniform temperature at the position where the temperature is recorded. In reality, internal temperature gradients are always present when the sample undergoes phase change at a fixed cooling or heating rate set by the DSC ("Dynamic mode"). This leads to enthalpy curves that are shifted along the temperature axis depending

on a melting or solidification experiment and is known as an artificial hysteresis [46, 48, 78]. This error could be decreased by using very low cooling and heating rates in the instrument. However this is traded off against an increased noise to signal ratio, which can induce more uncertainties [46]. A round robin test showed that a definition of a common test protocol was necessary for the dynamic mode to produce consistent results for the same PCM [45, 79].

An alternative would be to set the DSC to perform small step changes in temperature of the sample ("Step mode"). The enthalpy curve is then constructed from these temperature steps [46, 80]. The benefit is to decrease temperature gradients in the sample by allowing the sample to reach thermal equilibrium within each step. The trade-off is the additional time needed to perform the measurements compared to the dynamic mode.

It has also been proposed to inversely estimate the material parameter values based on a numerical model of the DSC experiment [46, 81].

Table 2.1: Literature overview of thermal characterization methods for PCMs

Method	Experimental Variant	Reference
DSC	Dynamic mode	[45, 79]
(mg-range)	Step mode	[46, 80]
	Inverse method	[46, 81]
T-History	Uninsulated sample holders	[82–86]
(g-range)	Insulated sample holders	[87–92]
Other		[42]

Moreover, many PCMs exhibit so called supercooling [12, 93, 94]. A supercooled state is given when the liquid phase is able to cool down below its phase change temperature (see Fig. 2.1). The liquid phase is then in a metastable state instead of solidifying. Once the thermodynamic barrier for solidification is overcome, a part of the liquid phase rapidly solidifies while releasing latent heat until the phase change temperature is reached and conventional solidification proceeds (so called recalescence [95]). Most of the experimental methods do not account for this phenomenon and have to be either simplified or adjusted [46, 85]. Depending on the PCM, supercooling may vary greatly [94]. While supercooling of a few degrees below the solidification temperature is common, salt-hydrates like sodium acetate trihydrate exhibit stable supercooling down to ambient temperatures despite a phase change temperature of 58 °C [96]. In a storage application, supercooling may introduce a risk that the PCM does not solidify within the available process temperatures. Such a case has to be avoided since its latent heat can then not be utilized.

Commercial PCMs usually contain additives to decrease supercooling by triggering solidification from nucleation sites [67]. When measuring PCMs, it is thus important to ensure that the sample size for such mixtures and heterogeneous PCMs is representative for the bulk material in the storage [78, 91, 97]. Since DSC devices utilize sample sizes in the range of milligrams, the supercooling phenomenon observed in DSC is usually more severe than in large scale applications [46, 97].

Finding a good approximation of the enthalpy curve that represents the material properties within the actual storage application is therefore necessary to explain and predict the PCM storage device performance. This involves measuring storage capacity, temperature range of phase change as well as supercooling behavior of the PCM.

In the literature, the so called T-History method has therefore gained considerable attention as a complementary method to DSC measurements. This is because sample sizes used in this method are increased by a factor of 1000 (sample mass in grams instead of milligrams). Since the introduction of its principle in 1999 [82], the method is still subject to development. No standardized method regarding setup and data evaluation exists [44]. Nevertheless, T-History measurements are frequently used to obtain reasonable estimates regarding storage capacity and supercooling behavior of larger PCM samples [97]. For certain PCMs, such as salt-hydrates, T-History is currently one of the recommended measurement methods listed in the quality assurance guidelines for PCM suppliers because of the above reasons [98]. In contrast, there is no recommendation on which of the experimental variants that are presented in the literature should be selected. This clear research gap for T-History is being addressed in the following sections of this thesis.

2.2 Discussion of the T-History method

The principle of the method is to subject both a PCM sample and a reference sample with known properties to a step change of the ambient temperature and to record their temperature responses (see Fig. 2.2). The experiment usually takes place within a temperature controlled enclosure, such as a climate chamber or water bath [44].

The enthalpy curve of the sample is then calculated from the recorded temperature data of sample and reference. Similar to DSC, a separate enthalpy curve is obtained for solidification and melting. Two main assumptions are made for the calculation:

1. It is assumed that the overall heat flow between the reference material and the ambient $\dot{Q}_{ref}$, and between the PCM and the ambient $\dot{Q}_{PCM}$, are equal for the same temperature difference $T - T_{amb} = T_{ref} - T_{amb} = T_{PCM} - T_{amb}$ [88]:

$$\dot{Q}_{ref}(T) = \dot{Q}_{PCM}(T) = \frac{1}{R_{th}(T)}(T - T_{amb}) \tag{2.3}$$

   In order to support this assumption in the experiment, the sample holders containing the PCM and reference are to be at least of the same geometries, yielding the same effective thermal resistance R_{th} in Eq. 2.3.

2. It is assumed that the measured temperature change over time is representative for the whole sample holder via a lumped model formulation for the sample or reference $k = \{\text{ref}, \text{PCM}\}$ and the sample holder tube:

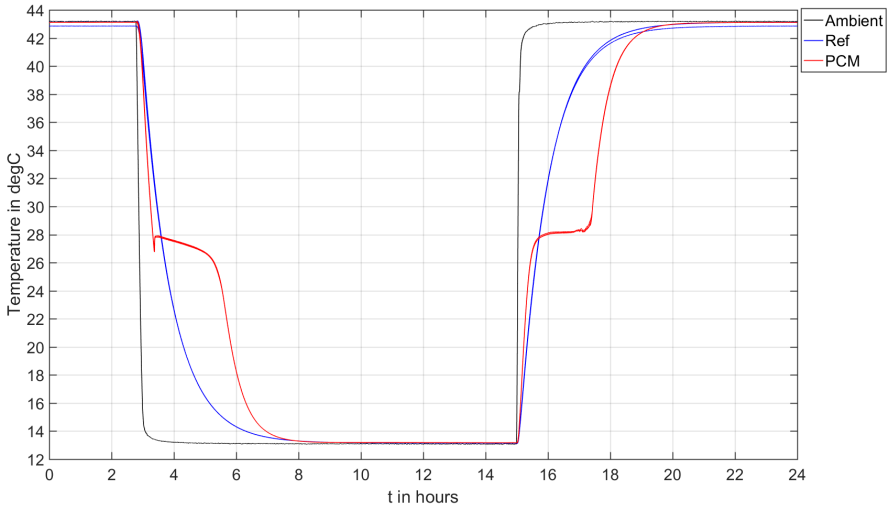

Figure 2.2: Example of measured temperature response from a PCM sample and reference due to ambient temperature step changes (from **Paper 2**). During cooling, a small degree of supercooling (ca. 1°C) is visible.

$$\dot{Q}_k(T) = (m^k \cdot {c_p}^k(T) + m^{tube,k} \cdot {c_p}^{tube}(T)) \cdot \left.\frac{\mathrm{d}T}{\mathrm{d}t}\right|_k \tag{2.4}$$

It is then possible to solve for the unknown effective heat capacity of the PCM ${c_p}^{PCM}(T)$ using the derivatives of the measured temperature responses of sample and reference:

$${c_p}^{PCM}(T) = \frac{m^{ref} \cdot {c_p}^{ref}(T) + m^{tube,ref} \cdot {c_p}^{tube}(T)}{m^{PCM}} \cdot \frac{\left.\frac{dT}{dt}\right|_{ref}}{\left.\frac{dT}{dt}\right|_{PCM}} - \frac{m^{tube,PCM} \cdot {c_p}^{tube}(T)}{m^{PCM}} \tag{2.5}$$

For convenience, the terms can be grouped together:

$$C_{ref}(T) = \frac{m^{ref} \cdot {c_p}^{ref}(T) + m^{tube,ref} \cdot {c_p}^{tube}(T)}{m^{PCM}} \text{ and } C_{tube,PCM}(T) = \frac{m^{tube,PCM} \cdot {c_p}^{tube}(T)}{m^{PCM}}$$

$${c_p}^{PCM}(T) = C_{ref}(T) \cdot \frac{\left.\frac{dT}{dt}\right|_{ref}}{\left.\frac{dT}{dt}\right|_{PCM}} - C_{tube,PCM}(T) \tag{2.6}$$

$$\Delta h^{PCM} = \int_{T}^{T+\Delta T} {c_p}^{PCM}(\tau) d\tau \tag{2.7}$$

Using these assumptions, a number of different experimental setups have been presented. A detailed overview is given in **Paper 1**. The setups can be grouped generally between uninsulated and insulated sample holders (Tab. 2.1).

For uninsulated sample holders, Mazo et al. [86] investigated the systematic errors that are present in the enthalpy over temperature curve caused by the above assumptions. With this setup it is important to consider that the heat flux is mainly determined by the forced heat transfer coefficient from the sample holder wall to the ambient. Badenhorst & Cabeza [99] showed that it is in practice very difficult to maintain this coefficient to be constant in a climate chamber, due to the circulation of the air inside the chamber. Therefore, the equal heat flux assumption may be invalid and leads to large errors when calculating the enthalpy curve.

For the alternative setup, an insulation layer around the sample holder dominates the heat transfer (or R_{th}) from sample and reference to the ambient in the experiment. The heat flux is then limited by the conductive heat transfer through the insulation [87, 88]. The work in **Paper 1** and **Paper 2** studies how the presence of the insulation affects the accuracy of the above assumptions. **Paper 1** presents a numerical study using a simulated experiment, while **Paper 2** presents a systematic experimental study using different setup variants.

2.2.1 Numerical study

The methodology used in **Paper 1** was to formulate a numerical model of a typical experimental setup as shown in Fig. 2.3. In the setup, it is assumed that the temperature sensors for the PCM and reference is located at the sample holder wall at $r = r_w$ (Fig. 2.3b). The experiment was simplified to a transient 1-D heat conduction model and implemented in COMSOL.

Solidification and melting experiments were simulated with a known enthalpy curve for both PCM and reference. The temperatures modeled at $r = r_w$ were then used with the assumptions in Eq. 2.3 and 2.4 to reconstruct the PCM enthalpy curve. It was found that neglecting the thermal mass of the insulation causes a systematic error in the enthalpy results. From the perspective of the insulation material, a transmittive and admittive heat flux can be defined according to Fig. 2.3b.

The heat flux that is assumed as equal in Eq. 2.3 corresponds to the transmittive heat flux of the insulation at the temperature sensor position. Thus, Eq. 2.3 should be more precisely expressed as:

$$\dot{Q}_{ref}^{transmittive}(T) = \dot{Q}_{PCM}^{transmittive}(T) \tag{2.8}$$

However, the numerical study shows that especially the transmittive heat flux is not equal while PCM and reference are cooling down or heated up during the experiment. The differences between the two simulated heat fluxes can be observed in Fig. 2.4 and 2.5. The sign of the heat flux is defined by $\frac{dT}{dt}$ in Eq. 2.4 depending on a heating or cooling case. The deviations can be summarized as follows:

- The initial transmittive heat fluxes immediately after the temperature step change can deviate considerably, when the PCM and reference have different thermal diffusivities. If possible, the temperature evaluation interval should therefore start from a value further from the initial temperature. In **Paper 2**

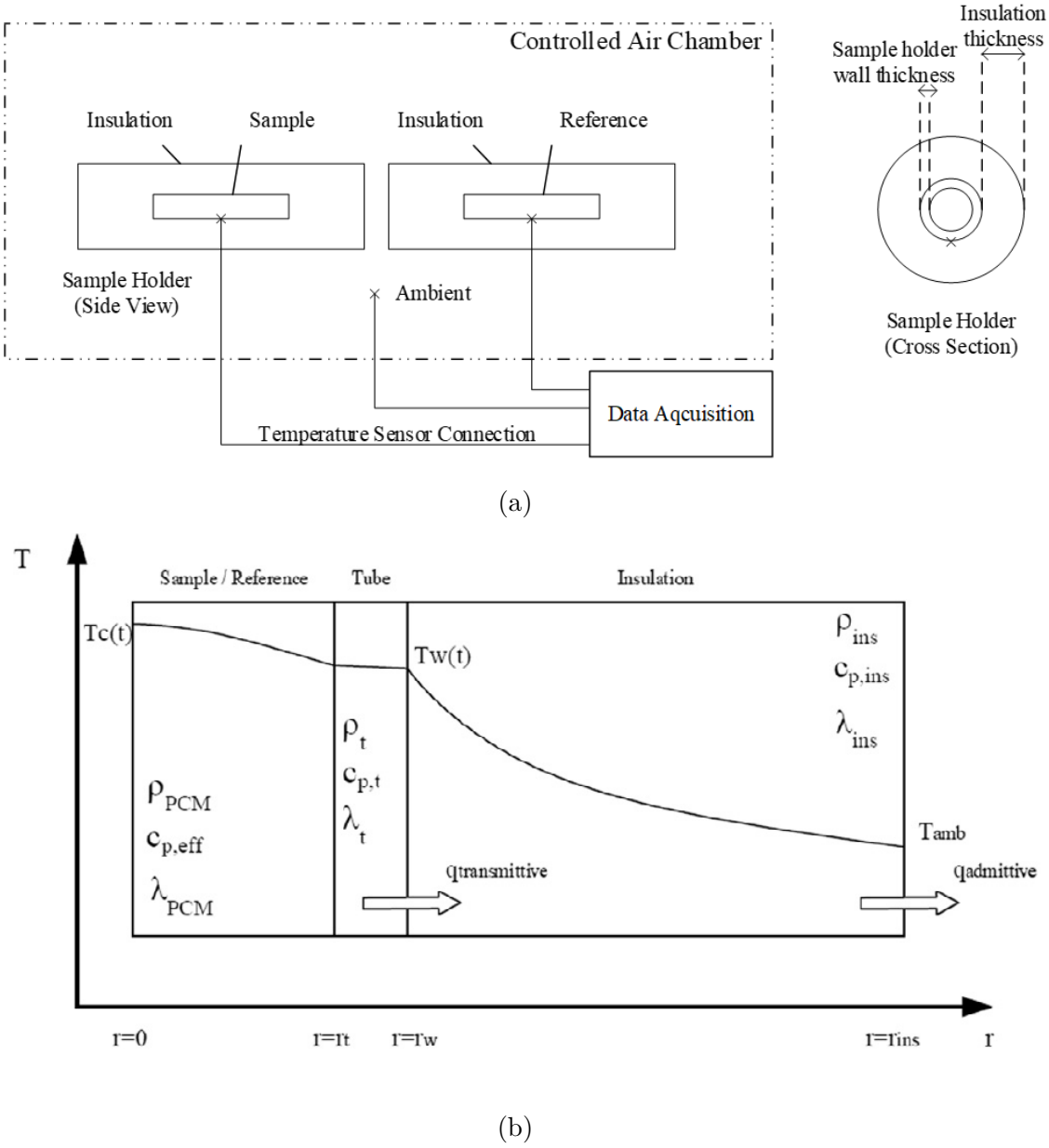

Figure 2.3: Illustration of the modeled T-History experiment using insulated sample holders (from **Paper 1**): (a) Principle sketch of the experimental setup and sample holder cross section. Temperature sensor locations are marked by 'x'. (b) Illustration of the corresponding numerical model in 1-D (solidification case) and the transmittive and admittive heat fluxes due to the insulation. $\dot{q}_{transmittive}$ is the heat flux density at the measurement sensor position at the sample holder wall.

it is shown that the suitable temperature interval is given by a region where $\left.\frac{dT}{dt}\right|_{ref}$ and $\left.\frac{dT}{dt}\right|_{PCM}$ is a linear function of the temperature.

- When the PCM undergoes phase change, $\dot{Q}_{PCM}^{transmittive}$ comes close to a steady state heat flux across the insulation with a constant T_{PCM} and T_{amb} at the

insulation borders. This near steady state heat flux deviates from $\dot{Q}_{ref}^{transmittive}$ and causes an underestimation of the latent heat portion in the enthalpy results.

- Temperature gradients exist in the PCM layer upon melting and solidification. The assumption of a uniform temperature from Eq. 2.4 therefore leads to an artificial hysteresis of the enthalpy temperature curve similar to DSC measurements.

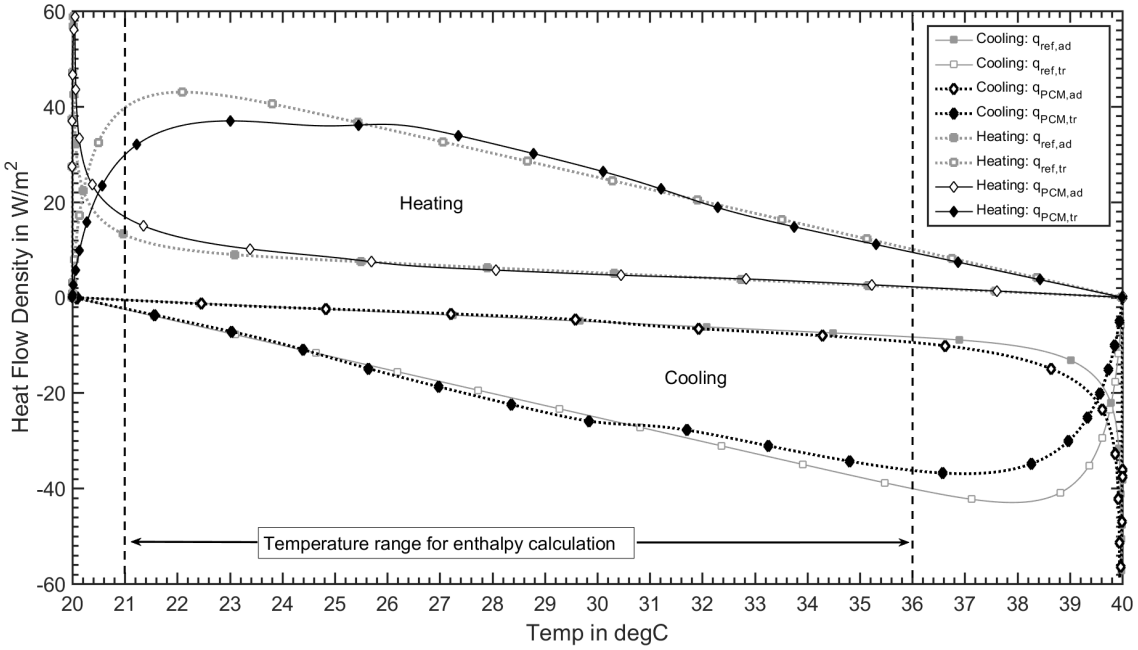

Figure 2.4: Simulated values of $\dot{Q}^{transmittive}$ and $\dot{Q}^{admittive}$ versus T for PCM and reference (from **Paper 1**).

The numerical study was carried out with variations of the insulation properties. The artificial hysteresis can be decreased with an increased insulation thickness due to reduced cooling/heating rates in the experiment. However, the first two deviations then increase due to a higher thermal mass of the insulation in the experimental setup. This was also observed by varying the insulation density in the model.

It was then shown that a correction of the systematic error should be ideally done. If the transmittive heat fluxes are known, a temperature dependent correction factor can be calculated and inserted into the original Eq. 2.6:

$$e(T) = \frac{\dot{Q}_{ref}^{transmittive}(T)}{\dot{Q}_{PCM}^{transmittive}(T)} \tag{2.9}$$

$$c_p'^{\,PCM}(T) = C_{ref}(T) \cdot \frac{1}{e(T)} \frac{\left.\frac{dT}{dt}\right|_{ref}}{\left.\frac{dT}{dt}\right|_{PCM}} - C_{tube,PCM}(T) \tag{2.10}$$

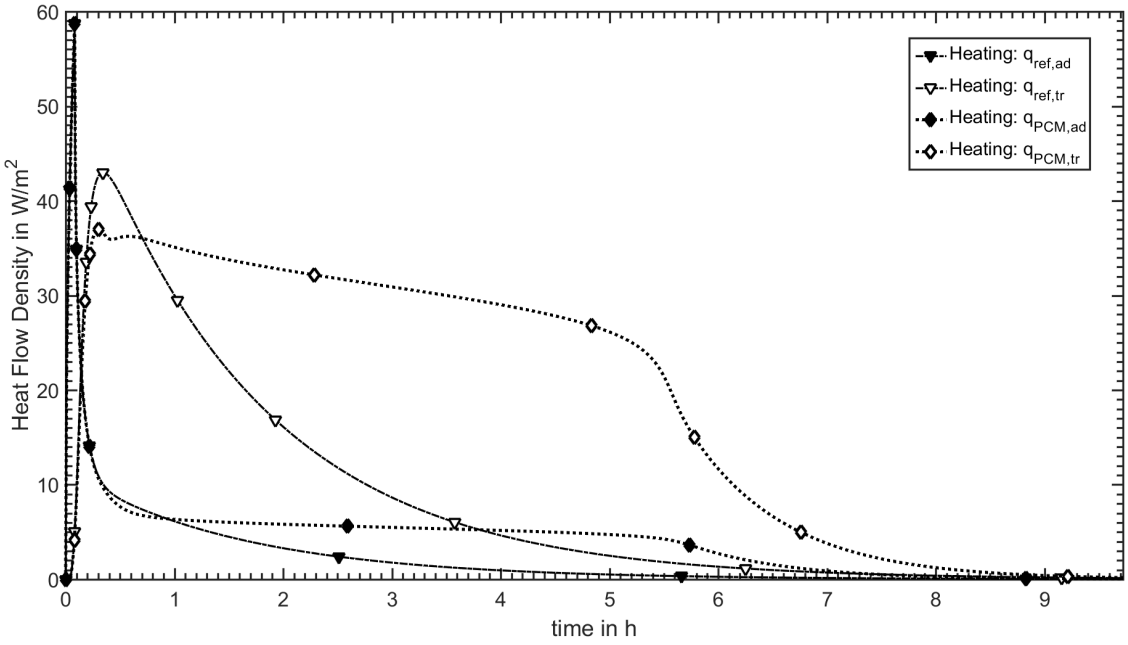

Figure 2.5: Simulated values of $\dot{Q}^{transmittive}$ and $\dot{Q}^{admittive}$ plotted over time for PCM and reference to illustrate the near steady-state heat flux for the PCM during phase change (from **Paper 1**).

However, if the heat fluxes are not known, it may be feasible to simply use a steady state assumption close to the phase change temperature in order to correct the latent heat portion. This would lead to a constant correction factor:

$$e^{simplified} = \frac{\dot{Q}_{ref}^{transmittive}(T_{PCM})}{\dot{Q}_{ref}^{steady-state}(T_{PCM})} = \text{const.} \tag{2.11}$$

More details about the scales of the error and the corresponding correction factors can be found in **Paper 1**.

Fig. 2.6 shows an example of the systematic deviation and corrected results. Within the parameters of the numerical study, the relative error was quantified as around 1 to 4 % for the chosen enthalpy difference. It was then concluded, that this predicted systematic error has to be verified and studied experimentally in order to place it in relation with other factors influencing the enthalpy results.

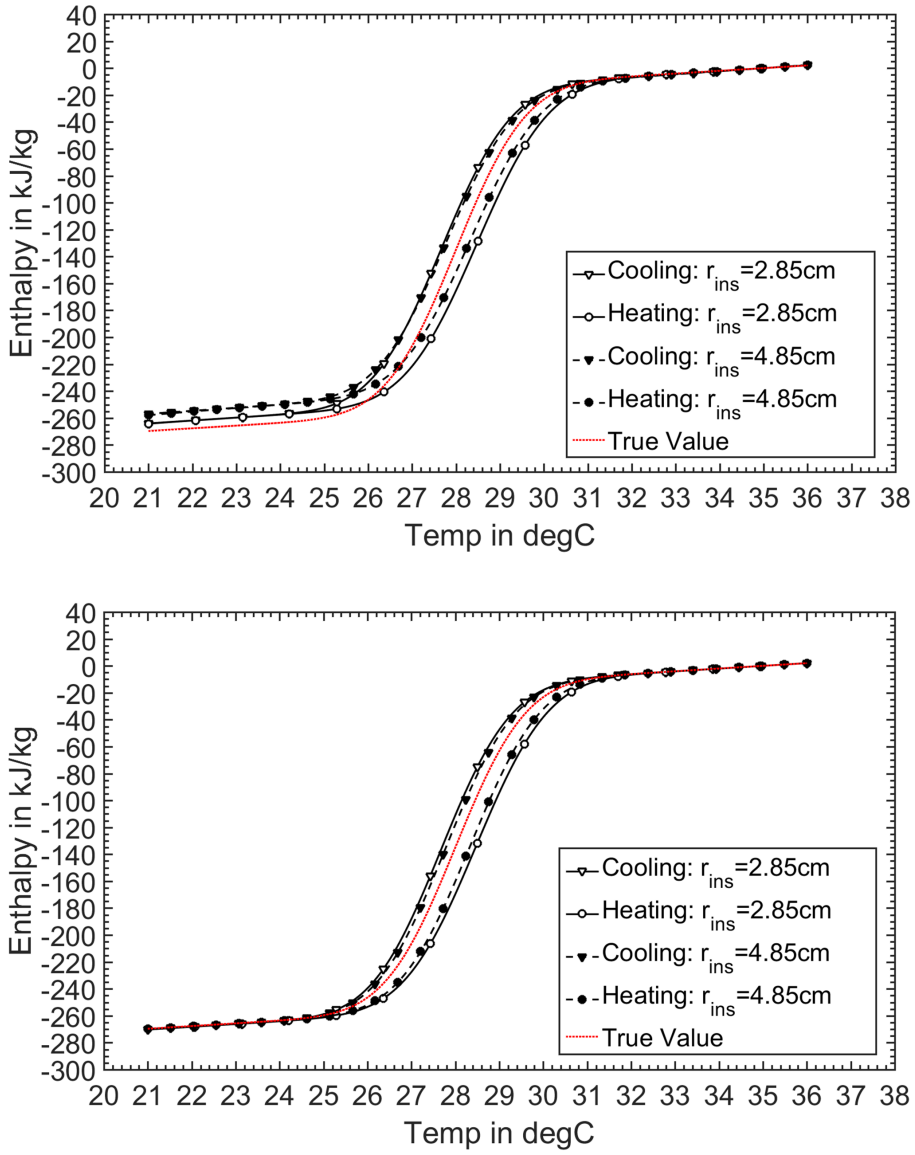

Figure 2.6: Results of uncorrected (top) and corrected (bottom) enthalpy versus temperature curves compared to the actual value (from **Paper 1**). Enthalpy values are normalized at 35 °C.

2.2.2 Experimental study

The experimental setup of Fig. 2.3a was implemented in **Paper 2** using different sample holder and insulation variants (see Fig. 2.7). Tab. 2.2 and 2.3 show a list of the considered experimental parameters. The work in **Paper 2** studies these variants in terms of 'accuracy' (influence of systematic errors) and 'precision' (reproducibility with repeated measurements) of the enthalpy versus temperature curve using a commercial paraffin (RT28HC) as PCM.

Table 2.2: Sample holder properties used in the experimental study of **Paper 2**. For setup B1 and B2 the same 15mm sample holder is used but with different insulation types.

Parameter	Setup A	Setup B1	Setup B2	
Sample holder (outer) diameter	10	15	15	mm
Insulation thickness	15.5	17	32	mm
m^{PCM} (RT28HC, paraffin)	4.2	10.1	10.1	g
m^{ref} (distilled water)	5.4	13.1	13.1	g
$m^{tube,PCM}$	25.2	46.8	46.8	g
$m^{tube,ref}$	25.0	46.9	46.9	g

Table 2.3: Climate chamber program for setup A and B (from **Paper 2**).

Parameter	Program I	Program II	
T_{amb}^{min} - T_{amb}^{max}	$18-38$	$13-43$	°C
$T_{pcm} \pm \Delta T$	28 ± 10	28 ± 15	°C
Duration of one complete heating and cooling cycle	$2 \cdot 12$	$2 \cdot 12$	h
Heating and cooling cycles performed	5	5	
Data acquisition interval	5	5	s

It was found that two important factors have to be considered in the data evaluation method in order to increase the precision of the enthalpy-temperature curve over subsequent measurements.

- Firstly, apparent noise of the temperature sensor may exist and is enhanced when formulating the first derivative $\frac{dT}{dt}$ [100, 101]. In general, a high noise to signal ratio is given when a fast data recording rate is chosen with respect to low heating/cooling rates in the experiment. Moreover, convection inside the sample holder during melting appears to be the reason for a significant amount of apparent noise recorded by the temperature sensor at the bottom of the sample holder. Fig. 2.8 shows the resulting movement of the solid phase during melting in a transparent sample holder. When liquid and solid phases are of different temperatures, a temperature sensor at the sample holder bottom would then record temperature fluctuations.

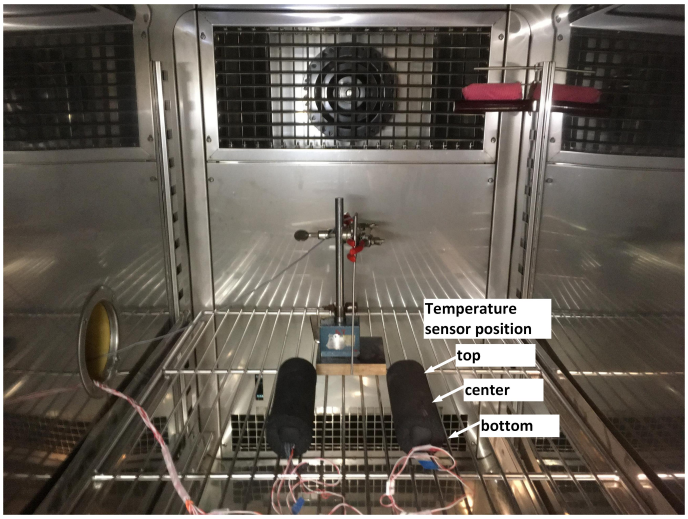

Figure 2.7: Photo of the experimental setup used in **Paper 2**. Exact experimental parameters are listed in Tab. 2.2. Three temperature sensors are used for each sample holder in order to evaluate the temperature uniformity of the climate chamber during the experiments.

- Secondly, the onset of solidification from a supercooled state causes negative values for $c_p^{PCM}(T)$ when using Eq. 2.6, due to $\left.\frac{dT}{dt}\right|_{PCM} > 0$ during this phase. It is proposed to treat this phase as an adiabatic case. For small degrees of supercooling, this assumption is likely reasonable, since the insulation ensures near-adiabatic conditions for a short period of recalescence.

A more robust data evaluation method is proposed in **Paper 2** that essentially involves smoothing out the noise. While it is likely that a new systematic error from smoothing is introduced, it is an acceptable trade-off, since it was possible to increase the reproducibility of the results within a single experimental variant to a degree, where the systematic deviations between the variants became quantifiable (see Fig. 2.9 and 2.10). Fig. 2.10 shows that within each setup, there is a small deviation between the enthalpy values determined from the three different temperature sensors. This is an error due to the temperature non-uniformity of the climate chamber. Moreover, experimental variant A obtains significant reduced enthalpy values due to a larger influence of the insulation thermal mass with respect to the PCM sample. This is in accordance to the numerical study of **Paper 1**.

Paper 2 also contains a study of the enthalpy uncertainties by propagating each input quantity uncertainty via the Monte Carlo method listed by the Joint Committee for Guides in Metrology [102]. It is shown that a larger sample mass in Setup B1 and B2 is preferable, since the effect of input quantity uncertainties is more dampened (Fig. 2.11).

Table 2.4 provides a summary of trade-offs between important experimental parameters in T-History.

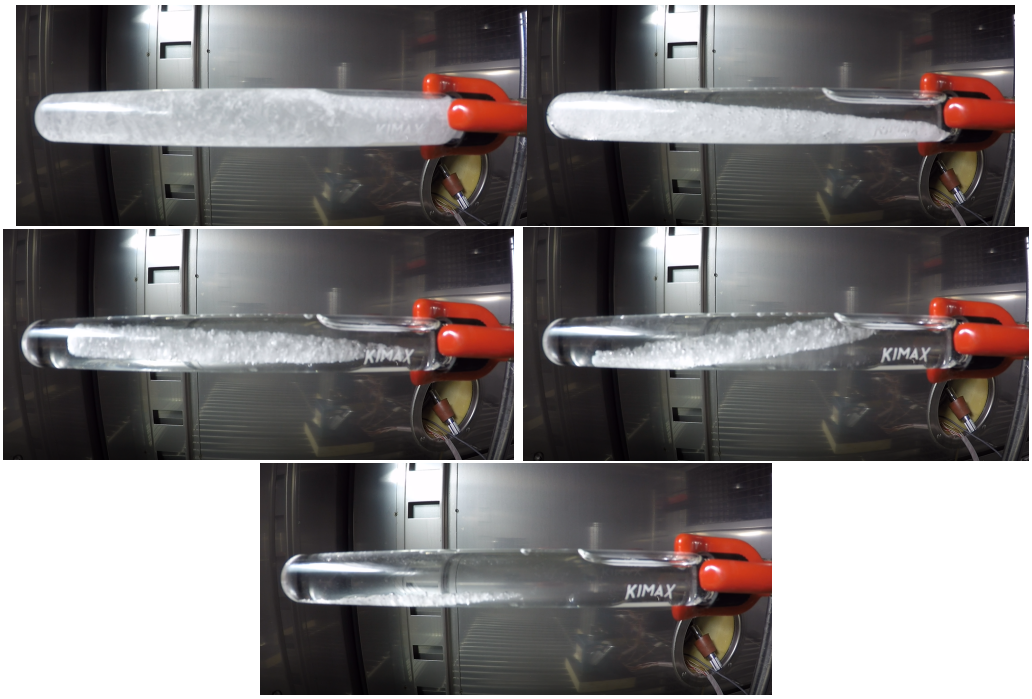

Figure 2.8: Photographs of solid phase movement of a commercial paraffin during melting (From top left to bottom right).

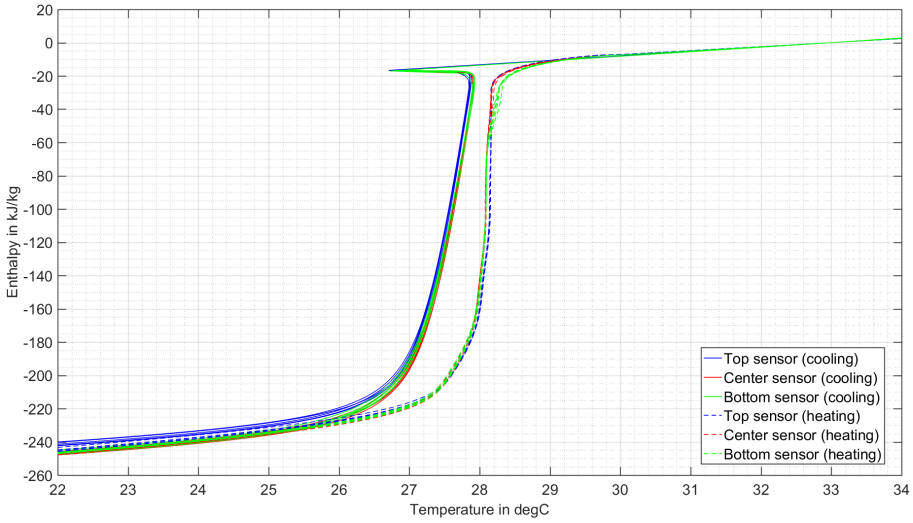

Figure 2.9: Enthalpy versus temperature curves for the Setup B2-I (from **Paper 2**). Five repetitive cycles are plotted with the same color depending of the sensor position. The enthalpy values are normalized at 33 °C.

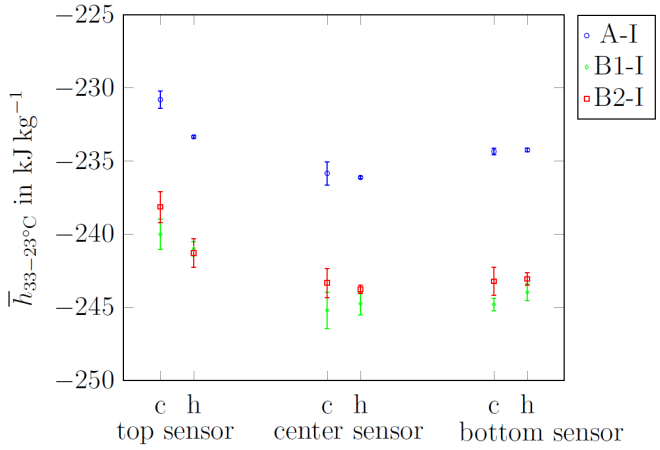

Figure 2.10: Mean enthalpy results and standard deviation for Setup A-I, B1-I and B2-I over five cycles for each sensor location (c: cooling, h: heating). Taken from **Paper 2**.

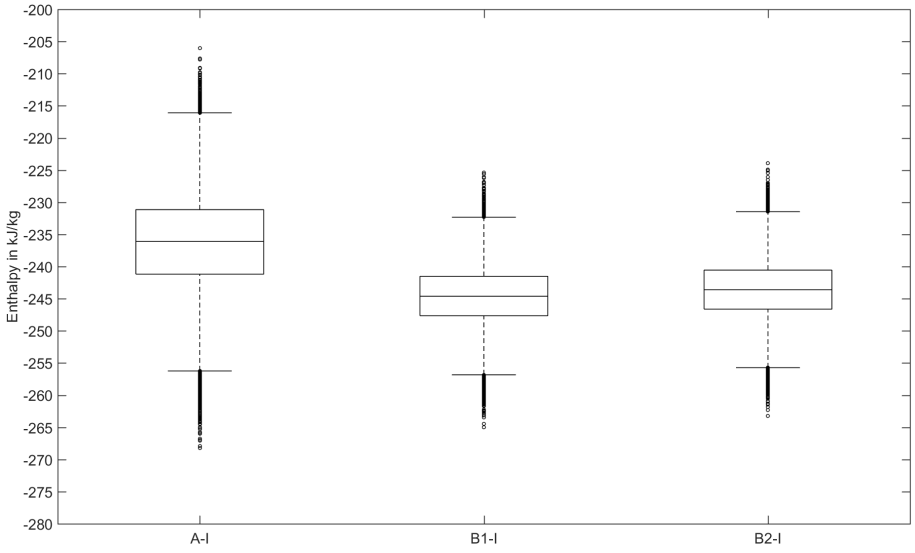

Figure 2.11: Box plots of $h_{33-23\,^{\circ}C}$ values from Monte Carlo simulations for setup A-I, B1-I and B2-I using $dT = 0.001\,^{\circ}C$ (center sensor position, heating cycle 1). Whiskers are extended to 1.5 times the interquartile range (IQR). Taken from **Paper 2**.

Table 2.4: Summary of studied experimental parameters and their influence regarding accuracy and precision of the T-history method.

Parameter	Motivation & Benefits	Cautions	Recommendations
Sample holder insulation	Increases precision and accuracy by making insulation the dominating heat transfer resistance in climate chamber; Decreases artificial hysteresis; Supports adiabatic assumption during solidification from supercooled state.	Causes systematic error using Eq. 2.3; Decreases suitable temperature interval for calculating enthalpy curve.	Use low thermal mass insulation whenever possible; Evaluate different combinations of sample holders and insulation sizes; A proposed methodology for correcting the systematic errors retrospectively is given by Brütting et al. [92].
Sample holder	Smaller sample holder diameter reduces artificial hysteresis; Larger diameter increases representativeness of sample size for a heterogenous PCM.	Higher influence of input quantity uncertainties on the enthalpy results with smaller sample mass possible; Long-term material compatibility between sample holder material and PCM has to be considered.	If temperature sensor is attached to the sample holder wall, the sample holder should be made of highly thermal conductive material (e.g. Copper); Evaluate different combinations of sample holders and insulation sizes.
Ambient temperature step change	Larger step changes increase the suitable temperature interval for calculating enthalpy curve.	Larger step changes lead to a larger artificial hysteresis.	Evaluate different step changes with the chosen setup to investigate suitable temperature intervals; Evaluate the climate chamber ability to maintain a constant ambient temperature after the step change; Time needed for the climate chamber to perform the step change should be considered as well.
Temperature sensor	Simple experimental setup using a single temperature sensor for each sample holder	Different heat flux may exist at different sample holder locations due to non-uniformity of climate chamber; Real and apparent noise has to be filtered out when forming the temperature derivative.	Choose temperature sensors using a fast response time; Check climate chamber for temperature uniformity using multiple temperature sensors for each sample holder; Test different smoothing techniques for noise removal.

2.3 Conclusions and outlook

In **Paper 1**, it is shown numerically that the common assumptions of the T-History method with insulated sample holders leads to systematic errors of the enthalpy versus temperature curve due to the influence of the insulation thermal mass in the experimental setup. **Paper 2** shows that several other experimental parameters also influence the accuracy and precision of the enthalpy versus temperature curve. A data evaluation method has been proposed to increase the precision of the method. While the improved methodology likely does not allow the measurement of accurate absolute values of the enthalpy curve, it can be used to compare relative changes of the results due to different setup parameters since the precision of the method is high enough. Specifically, it has been found that systematic differences in the enthalpy values and artificial hysteresis of the studied variants generally depend on the chosen ratio of sample mass and insulation layer in the setups. Together with an uncertainty analysis it is shown that Setup B1 and B2 yield a more acceptable trade-off between measured enthalpy value and artificial hysteresis over Setup A. This can be attributed to the larger sample mass in the former setups.

Future work should continue to systematically evaluate the suitability of different T-History variants. Thus, it is recommended to perform T-History round-robin tests, as it has been done with DSC, in order to standardize the method. This involves both the experimental setup as well as different data evaluation techniques. Moreover, the effect of supercooling in thermal analysis methods should be taken into account more rigorously. A recent follow up work by Brütting et al. [92] shows that it is possible in practice to perform heat flux correction retrospectively for insulated T-History setups as predicted in **Paper 1**. Another interesting option would be to replace the temperature sensors in the setup with dedicated heat flux sensors, so that the transmittive heat flux and correction factors from **Paper 1** in can be determined rigorously. Moreover, the enhancement of noise when forming the temperature vs. time derivate is avoided.

Obtaining an accurate representation of the PCM properties during phase change is therefore still an active field of research. It can be done either by developing new [42, 43, 46] or standardizing existing methods [45, 79]. It is worth noting that characterizing other thermal properties of PCM, such as thermal conductivity or thermal stability is also still ongoing and many different approaches have been proposed [37, 103].

Chapter 3

Laboratory-scale study of a commercial Salt-Hydrate TES

3.1 Background and motivation

This chapter summarizes the work done in **Paper 3**. It investigates the same storage device design as in **Paper 4** but on a laboratory scale.

As mentioned in section 1.3, a PCM TES using a salt-hydrate as PCM is selected for the case study. For this PCM class, the phenomenon of supercooling and phase separation/incongruent phase transition are known practical problems [35, 67, 94, 104]. Most past studies on the performance of salt-hydrates and other PCMs have been done separately either on material scale, e.g. using DSC measurements, or on device scale using prototypes. In practice, it is desirable that the PCM properties measured with small scale samples is also representative to its behavior in the actual storage device. However, the few existing works that compared measurements done on material and device scales showed different results.

Both Rathgeber et al. [97] and Zondag et al. [105] showed that the salt-hydrate $MgCl_2 \cdot 6H_2O$ has a smaller degree of supercooling when increasing the sample size from DSC/T-History to device scale. A similar observation was made by Xu et al. [106] using commercial sodium acetate trihydrate as PCM. Since nucleation from a supercooled state is seen as a stochastic process, it is expected that the probability of nucleation increases with larger amounts of PCM. Work done by Englmaier et al. [107] shows that supercooling can even be a desired property for heat storage applications, since stable supercooling at ambient temperature can be utilized to decrease thermal losses between charging and discharging occasions.

The term 'phase separation' is generally used when the initial PCM mixture changes in composition. 'Incongruent phase transition' (or more commonly 'incongruent melting') on the other hand describes the specific phenomena when phases of different material compositions precipitate from the original mixture upon continued melting and solidification cycles [12]. When the new phases melt and solidify outside of the process temperature range, a decrease of overall storage capacity can be measured. Since this is an intrinsic material problem, it can already be observed with thermal cycling on material scale [26, 27, 35]. A phase diagram can be used to

ensure that the initial PCM mixture changes phase congruently [12]. The majority of available literature regarding these phenomena are based on work performed on material scale [35]. Existing investigations on device scale using salt-hydrates as PCMs show a significant deterioration of storage performance due to phase separation. In [105] for example, a drop in storage capacity compared to DSC results has been reported in a shell and tube storage prototype using $MgCl_2 \cdot 6H_2O$. For sodium acetate trihydrate, phase separation has also been observed using bottled containers [108] and in a prototype with macro-encapsulated PCM cylinders [106]. In the latter work, four T-History measurement cycles are presented for which a phase separation of the PCM is not apparent. Decreased melting times in the top parts compared to the bottom parts of a storage have also been reported [105, 109], which may indicate a change in material composition of the PCM occurred.

From this study of recent literature, it is therefore clear that the chosen storage design in the case study has to be investigated regarding its performance using a laboratory prototype. Especially since both supercooling and phase separation introduce the risk that the PCM does not solidify and melt within the application temperatures.

3.2 Experimental study of the laboratory scale PCM TES

An experimental study of a laboratory unit of the chosen PCM TES is presented in **Paper 3**. The goal of the study is to predict the storage performance within the actual process boundaries. Therefore, the following aspects were considered in the experiments:

- Process temperature ranges are chosen according to the actual application.
- Solidification/melting (charging/discharging) times do not exceed a daily operation cycle.
- Experiments are performed over multiple cycles.
- Repeatability of the experiments are studied.
- Useful power and storage capacity are determined either by process requirements on the storage outlet temperature and/or by the available solidification/melting time.
- Comparison with T-History samples.

3.2.1 Description of the laboratory setup

Fig. 3.1a shows a photograph of the lab scale PCM TES unit that was constructed in **Paper 3**. The storage container is filled with 168 kg of the salt-hydrate SP11. According to the manufacturer, the PCM has a phase transition temperature of about 11 °C and a theoretical storage capacity of $Q_{max} = 4.92\,\mathrm{kW\,h}$ for the application temperature range of 10 °C. This translates to a theoretical possible storage density of $\delta_{max} = 36.21\,\mathrm{kW\,h\,m^{-3}}$, based on the PCM volume. The PCM is charged and

discharged via a heat exchanger that is submerged into the PCM. It is built from 18 capillary tube mats made from polypropylene random copolymer pipes. Each mat has 44 vertical capillary tubes, of which 22 each are parallel connected to the supply and return pipe of the mat, respectively. The flow distribution in a mat follows a U-shape through these parallel connected capillaries as shown in Fig. 3.1b.

The supply and return pipes are located at the top of the heat exchanger. These serve as storage inlet and outlet connection for the heat transfer fluid (HTF) that is used to solidify and melt the surrounding PCM. An overview of the storage specifications is given in Tab. 3.1.

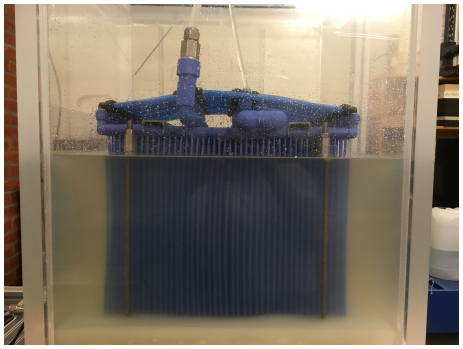

(a) Photo of PCM TES showing the heat exchanger and surrounding SP11.

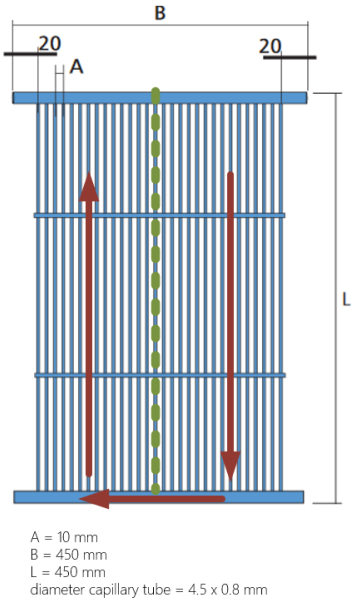

(b) Capillary tube mat geometry of the laboratory prototype [74].

Figure 3.1: Illustration of laboratory PCM TES from **Paper 3**.

Table 3.1: Laboratory PCM TES specifications (from **Paper 3**).

Property	Value	Comment
m_{PCM}	168 kg	
V_{PCM}	125.37 L	
ρ_{PCM}	1340 kg m^{-3}	Manufacturer value at 20 °C
T_{PCM}	11 K	Manufacturer value
N_{mats}	18	
d_{mats}	25 mm	center-center distance between mats
d_{tubes}	10 mm	center-center distance between tubes in each mat
N_{tubes}	792	396 parallel connected
V_{HEX}	10.5 L	External volume of mats in contact with PCM
V_{TES}	135.87 L	$V_{PCM} + V_{HEX}$
Q_{max}	4.92 kW h	Manufacturer estimate for the application temperature difference of ca. 10 °C
δ_{max}	36.21 kW h m^{-3}	$\frac{Q_{max}}{V_{TES}}$

The storage is connected to a test setup shown in Fig. 3.2. A thermostatic bath circulator provides a constant HTF inlet temperature to the storage through a plate heat exchanger. The bath is programmed to alternate its temperature between 7-17 °C every 12 hours and consecutive charging and discharging cycles are performed over this time interval, respectively. Table 3.2 gives an overview of the studied experiments and their parameters. Testing was done with three different mass flow rate ranges set via the pump and metering valve. The temperature of the PCM inside the storage is monitored using 15 PT100 sensors distributed over 10, 20 and 30 cm depths, which corresponds to 'top', 'middle' and 'bottom' parts of the PCM TES, respectively. More details of the measurement equipment are given in **Paper 3**.

Table 3.2: Overview of experiments (from **Paper 3**).

Experiment	$\dot{m}$ (kg min^{-1})	T_{bath} (°C)	No. of cycles (melting/solidification)
HF 1	1.375 ± 0.13	$7 - 17$	(5/4)
HF 2	1.375 ± 0.13	$7 - 17$	(8/7)
HF 3	1.375 ± 0.13	$7 - 17$	(17/16)
MF	1.0 ± 0.15	$7 - 17$	(17/16)
LF 1	0.8 ± 0.1	$5 - 16$	(4/3)
LF 2	0.65 ± 0.05	$7 - 17$	(10/9)

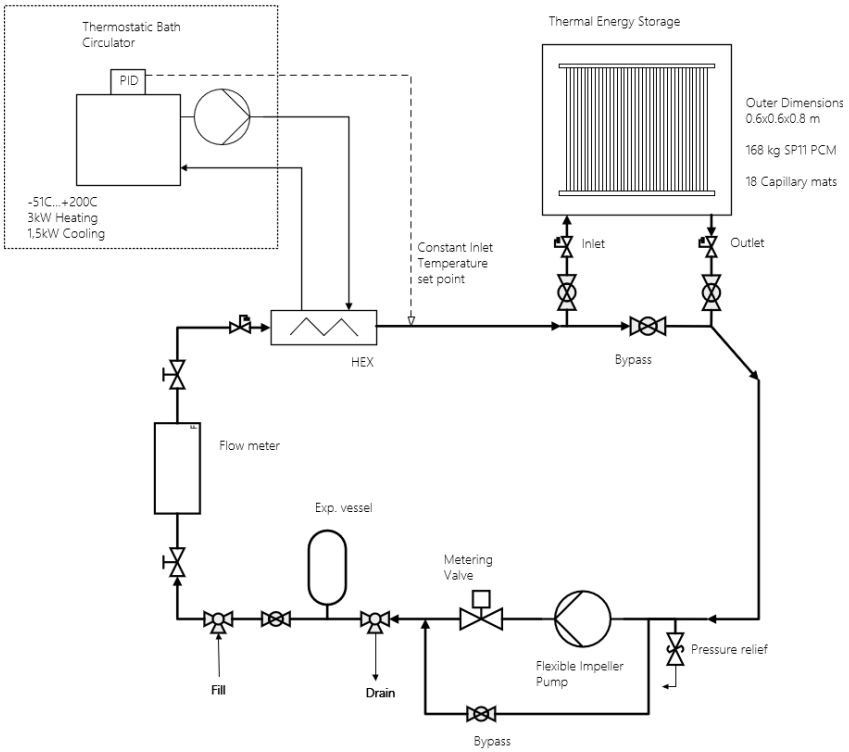

Figure 3.2: Sketch of the experimental setup used in **Paper 3**.

The storage power (W) and capacity (kW h) over each cycle were calculated from the measured storage inlet and outlet temperature and mass flow rate according to Eq. 3.1 and 3.2. The data recording rate was set to 10 s.

$$P(t) = \dot{m}_{HTF}(t) \cdot c_p \cdot (T_{in}(t) - T_{out}(t)) \tag{3.1}$$

$$Q(t) = \int_0^t \left|P(t')\right| dt' \tag{3.2}$$

For discharging, a cutoff condition is furthermore defined for the PCM TES outlet temperature of $T_{out}(t = t^*) = 14\,°\text{C}$. This condition represents the maximum allowed temperature of the process, for which the storage supplies cold energy. The condition can also be defined, for example, when the power for operating the auxiliary equipment (such as pumps) exceeds the power output of the storage. The utilizeable storage capacity during discharging is then the capacity discharged from the storage until the cutoff condition is reached (Q_{eff}). A capacity effectiveness η_{eff} (-) can also be defined as a ratio of Q_{eff} and the theoretical maximum storage capacity from the PCM manufacturer [76].

$$Q_{eff} = \int_0^{t^*} |P(t)| dt \tag{3.3}$$

$$\eta_Q = \frac{Q_{eff}}{Q_{max}} \tag{3.4}$$

An effective storage density (kW h m^{-3}) is then given by:

$$\delta_{eff} = \eta_Q \cdot \delta_{max} \tag{3.5}$$

3.2.2 Results of laboratory storage

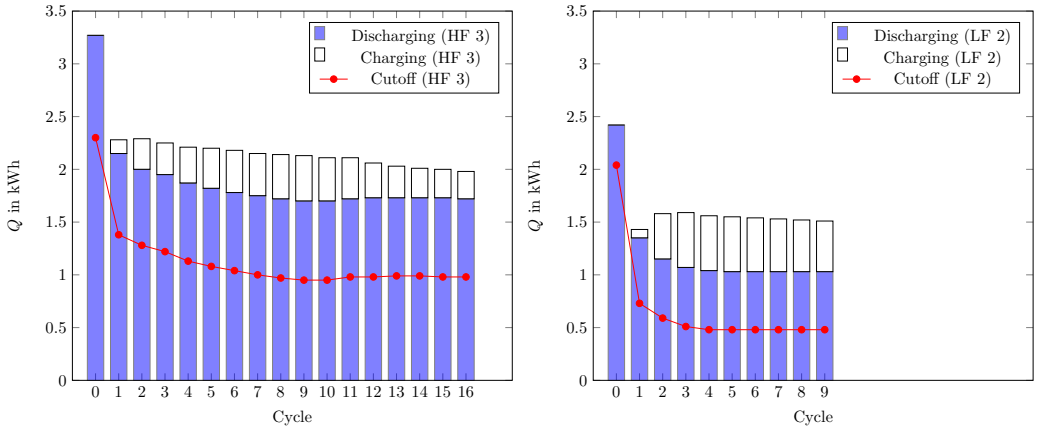

(a) HF 3 (b) LF 2

Figure 3.3: Measured discharging and charging capacities over subsequent cycling for experiments HF 3 and LF 2 (from **Paper 3**).

The experiments were analyzed starting from an initially solidified (charged) state. The first melting (discharging) occasion was denoted Cycle 0, followed by

solidification and melting Cycle 1. Up to 16 cycles were performed for an experimental series. A comparison between the experiments with the same mass flow rates (HF 1-3) showed good repeatable results (see **Paper 3**). The major observation was that for all experiments listed in Tab. 3.2, a decrease of storage capacity with subsequent charging and discharging cycles was observed. This is exemplary shown in Fig. 3.3 for the experiments HF 3 and LF 2.

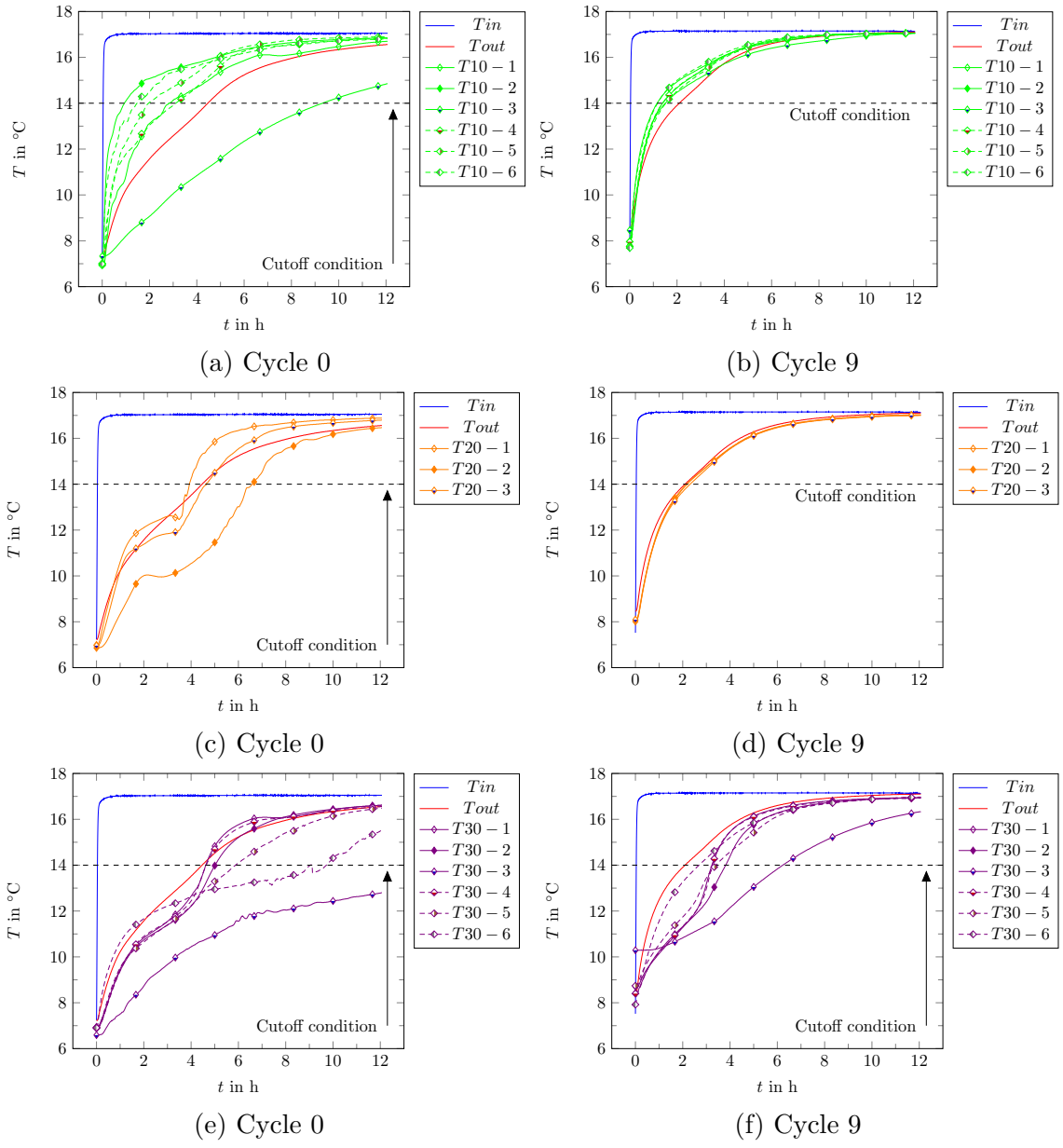

(a) Cycle 0 (b) Cycle 9

(c) Cycle 0 (d) Cycle 9

(e) Cycle 0 (f) Cycle 9

Figure 3.4: HF 3: Comparison of PCM temperature for melting Cycle 0 and 9. T10, T20 and T30 refer to individual temperature sensors at 10, 20 and 30 cm depth in the PCM TES, respectively (from **Paper 3**).

A portion of the storage capacity drop from the first solidification cycle likely stems from the limited charging time of 12 hours in the experiment. However, the temperature sensor readings in Fig. 3.4 show that the storage capacity decrease is

largely a consequence of the top and middle parts of the PCM TES storing only sensible heat.

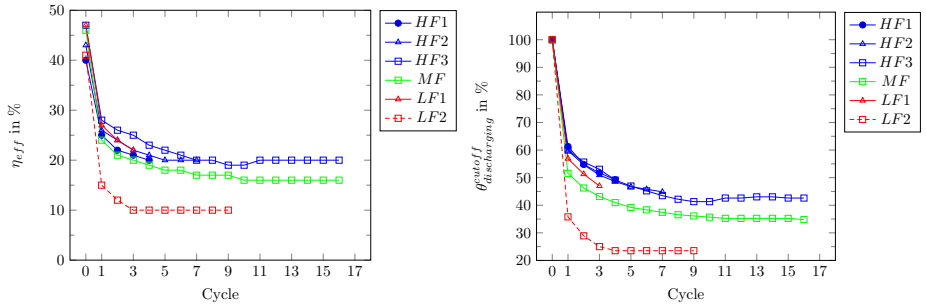

(a) Capacity effectiveness

(b) Relative values: $\theta^{cutoff}_{discharging} = \frac{Q^{cutoff}_{discharging}}{Q^{cutoff}_{discharging}(Cycle\ 0)}$

Figure 3.5: Measured discharging parameters over subsequent cycling (from **Paper 3**).

This storage capacity decrease causes also a significant drop in capacity effectiveness starting from melting/discharging Cycle 1, since the cutoff temperature is reached earlier (Fig. 3.5a). In Fig. 3.5b, the measured cutoff capacities for each discharging cycle is related to the measured first melting occasion (Cycle 0) using the parameter θ. It can be seen that the useful storage capacity decreases down to 45-25 % depending on the mass flow rate setting. Due to the upper PCM parts not solidifying or melting, the power output of the storage also decreases (Fig. 3.6).

The observation that the top and middle sections do not take part in solidification and melting can also be confirmed visually as shown in Fig. 3.7.

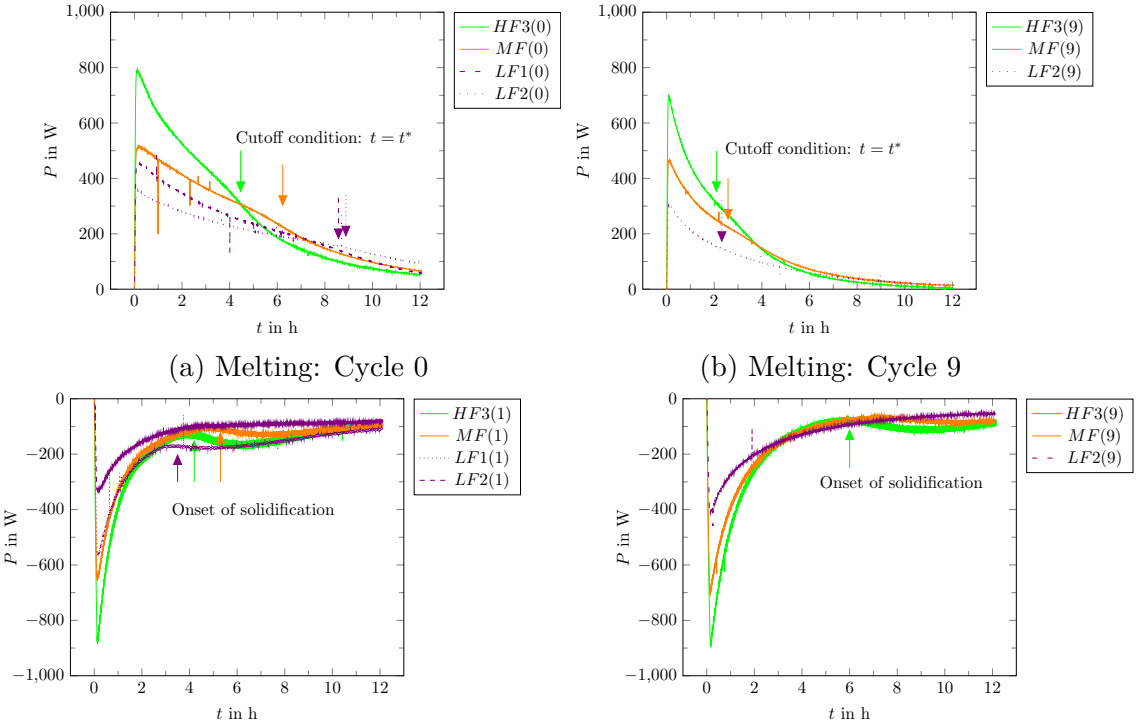

(a) Melting: Cycle 0

(b) Melting: Cycle 9

(c) Solidification: Cycle 1

(d) Solidification: Cycle 9

Figure 3.6: Charging and discharging power for HF 3, MF and LF 2 for melting (Cycle 0 and 9) and solidification (Cycle 1 and 9). Taken from **Paper 3**.

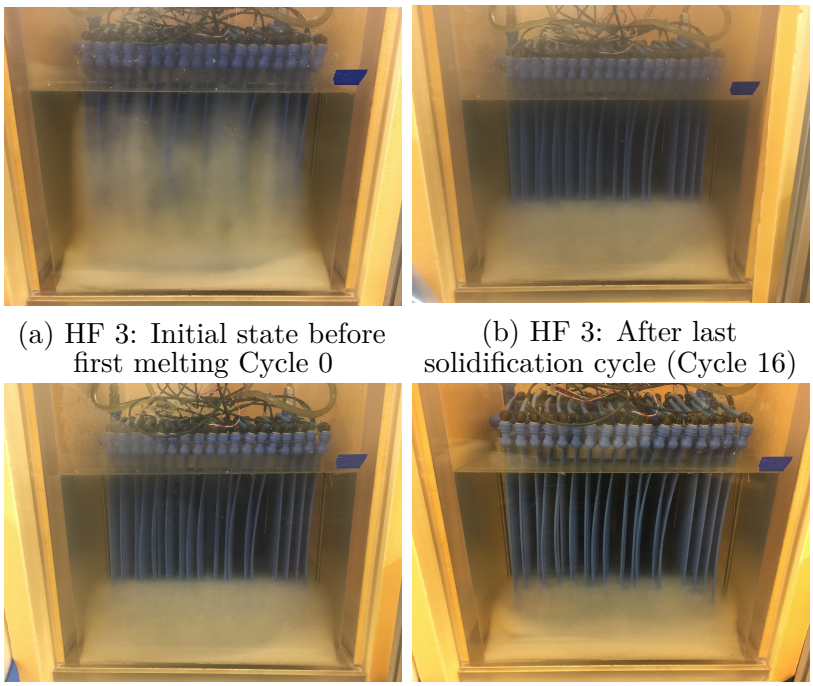

(a) HF 3: Initial state before first melting Cycle 0

(b) HF 3: After last solidification cycle (Cycle 16)

(c) HF 3: After last melting cycle (Cycle 16)

(d) LF 2: After last melting cycle (Cycle 9)

Figure 3.7: Photos of PCM TES for HF 3 and LF 2 (Insulation removed to take photo). Taken from **Paper 3**.

3.2.3 Discussion of observed phase separation

T-History experiments using the methodology described in **Paper 2** were performed on samples taken from two different storage heights before and after experiment HF 3. It was possible to confirm that the PCM exhibited increased phase separation and supercooling that caused the drop in storage capacity (see Fig. 3.8). From the samples taken before cycling, it can already be seen that the liquid PCM did not consist of a uniform mixture at the start. The increased degree of supercooling of the top sample explains why the top parts of the storage did not solidify in the first solidification cycle. The samples after cycling showed a systematic shift of supercooling and phase change temperature towards lower temperatures. Thus, solidification and melting were not anymore possible within the available process temperatures. Additionally, these samples showed a reduction in storage capacity over the studied temperature range.

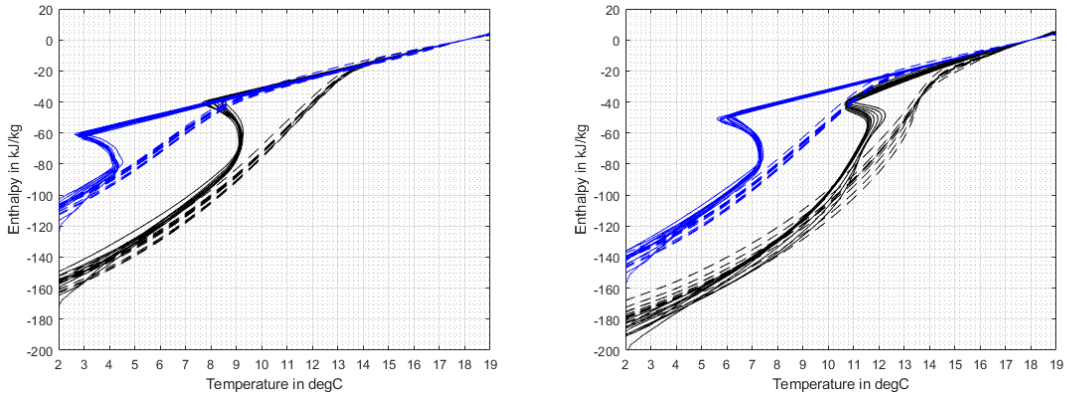

(a) Top Sample (from 1/3 height at 13 cm depth)

(b) Bottom Sample (from 2/3 height at 27 cm depth)

Figure 3.8: Enthalpy versus temperature curves of samples taken from the same tank location before (color: black) and after (color: blue) cycling. Each sample was measured using 11 melting (dashed line) and solidification (solid line) cycles. Normalization of enthalpy values at 18 °C. Taken from **Paper 3**.

An important result here is that each PCM sample by itself does not show a visible degradation during the performed 11 T-History cycles. Therefore, incongruent phase transition of the initial PCM mixture itself appears not to be the reason for the decrease of storage capacity in the storage. Rather, it can be explained that different liquid phases are initially present in the PCM. Given the design of the storage, the liquid phases can separate across the storage height. When these liquid phases solidify outside of the application temperature range, the overall storage capacity decreases, since only sensible heat is stored in these parts.

While the limited 12 hour solidification time likely also contributes to a decrease of storage capacity starting from the first solidification cycle, the T-History measurements of the samples and the photographs of the tank provide evidence that the majority of the capacity decrease is explained by the phase separation of the PCM. Incongruent phase transition during the formation of these new phases may be still possible and should be investigated on more samples.

Additionally, a larger storage capacity decrease was observed at lower mass flow rates. This indicates a possible connection between the rates of phase transition and phase separation. It should be investigated if it is possible to operate the storage in such a way that a higher rate of solidification and melting than phase separation yields a more stable performance. However, when the phase separation occurs in the liquid phase, a degradation of the material also needs to be prevented while the PCM TES is in an idle melted/discharged state.

Another important result is that phase separation can be reversed relatively easy using the known theory described in the literature [12]. It is achieved by first heating up the PCM inside the tank to 45 °C. At this temperature most of the solid PCM phases transitioned back to a liquid state and the PCM in the tank can be mixed mechanically. The good repeatability of the experiments indicates that the initial PCM mixture was restored reasonably well using this procedure.

3.3 Conclusions and outlook

In **Paper 3**, a laboratory PCM TES has been studied using similar working conditions as in the intended full scale installation. It was found that phase separation and supercooling of the commercial salt-hydrate yielded a storage capacity decrease over repeated cycling. T-History measurements on PCM samples from the storage showed a systematic shift of phase change temperature, storage capacity and a higher degree of supercooling for different locations of the storage after cycling. It is likely that the original PCM mixture is able to separate into different liquid phases across the vertical height of the storage tank. In future work the exact chemical composition of the PCM should be analyzed to confirm this observation.

The work presented in this chapter also revealed that it is not possible to predict the performance of an actual storage device using T-History measurements alone. This is because of the large difference in the geometrical aspect ratios of the T-History sample holder compared to the storage. The material is restricted in vertical height by the sample holder geometry compared to the storage tank. Interestingly, a prior testing by the storage supplier involving a vertical PCM cylinder also did not predict the phase separation. Therefore, it is clear that testing using a representative storage prototype is essential to predict the actual storage performance. In the future, it is desirable to create a testing methodology on material scale that can also assess material properties like supercooling and phase separation before building a storage prototype.

The impact of phase separation can be likely mitigated using appropriate measures in the material and storage design. The PCM could be geometrically restricted or an additive can be added that prevents movement of liquid phases. In this case, the latter solution was chosen by the manufacturer as described in the next chapter.

Chapter 4

Techno-economic evaluation of a full-scale PCM TES

4.1 Background and motivation

Despite the high research interest in recent years, real-world PCM TES installations have rarely been reported or analyzed. Most of the work done has been either on material or laboratory scale [3, 16, 22]. Therefore, it is of interest to analyze the reasons behind the wide gap between the amount of prototype studies and actual PCM TES applications. Addressing these may lead to a higher real word penetration of PCM storages.

On one hand, upscaling a storage prototype from laboratory conditions to real scale processes is accompanied by uncertainty factors, since testing of PCM TES is generally not standardized (as shown in the previous chapter). On the other hand, it was found that economic analysis of existing PCM TES are not commonly performed.

The technical and economic performance of a PCM TES has to be moreover placed in context with existing storage technologies. Recent working groups in the IEA ECES Annex 30 and 31 have started to define common key performance indicators (KPI) for sensible and latent heat as well as thermo-chemical energy storages [59, 60]. A comparison of different storage case studies for building applications by Del Pero et al. [61] shows that there is a discrepancy among the availability of different KPI. Technical KPI's such as storage capacity and achievable power are usually reported, as they can be obtained from laboratory prototypes. KPI's, which quantify the economic performance of a PCM TES are, however, usually missing. In [61], only one out of ten case studies contained an economic estimate. Moreover, also recent literature on existing full scale PCM TES installations have not reported an economic analysis [71, 72].

In contrast, earlier works analyzing full scale ice/snow storage installations showed that the economic benefits can only be quantified if at least the following points are included [110–112]:

- Actual technical performance of the storage within the process.
- Control strategy of the storage within the process.

- Energy price tariff of the process.

It is clear that economic key performance indicators provide essential information needed for decision making. The lack of this information makes it not possible to justify an investment decision for PCM TES and is likely a major reason for the low number of actual storage installations.

To address this gap, a techno-economic analysis of a full scale PCM TES storage is presented in **Paper 4**. A methodology is proposed on how the economic feasibility can be estimated for the presented case study. The storage is first tested regarding its technical performance. This data is then utilized to estimate the achievable economic performance of the storage.

4.2 Determining KPIs

The storage presented in **Paper 4** is a larger version of the PCM TES tested in **Paper 3**. The PCM TES is installed in an office building (11 700 m^2 of floor area) located in Gothenburg, Sweden (Fig. 4.1b). The installed capacity is estimated by the manufacturer to be $Q^0_{TES} = 275\,\text{kW h}$ for the given application. The capillary tube mats are scaled up to the dimensions of Fig. 4.1a and a total of 100 mats are connected to a heat exchanger that is submerged into 7000 L of the PCM SP11, which is a factor 55.8x increase of PCM volume compared to the laboratory storage. Fig. 4.2 shows the capillary tube arrangement within and between two mats. The storage has a total exterior volume of 11 200 L that are mostly defined by the PCM-, heat exchanger- (HEX) and insulation (INS) volume (Tab. 4.1).

In order to prevent phase separation of SP11 that was observed in the laboratory storage, three weight percent of the superabsorbent polymer (SAP) sodium polyacrylate (brand name: FAVOR PAC) was added to the PCM by the storage supplier.

Table 4.1: Full scale PCM TES specifications (full table available in **Paper 4**).

Property	Value	Comment
V_{PCM}	7000 L	Fill height of 1.6 m
ρ_{PCM}	1340 kg m^{-3}	Manufacturer value at 20 °C
m_{PCM}	9380 kg	
T_{PCM}	11 K	Manufacturer value
Q^0_{TES}	275 kW h	Manufacturer specification
V_{HEX}	481 L	External volume of mats in contact with PCM
V_{TES}	7481 L	$V_{PCM} + V_{HEX}$
V_{INT}	7862 L	Total internal tank volume
V_{INS}	2776 L	Insulation volume
V_{EXT}	11 200 L	Exterior volume

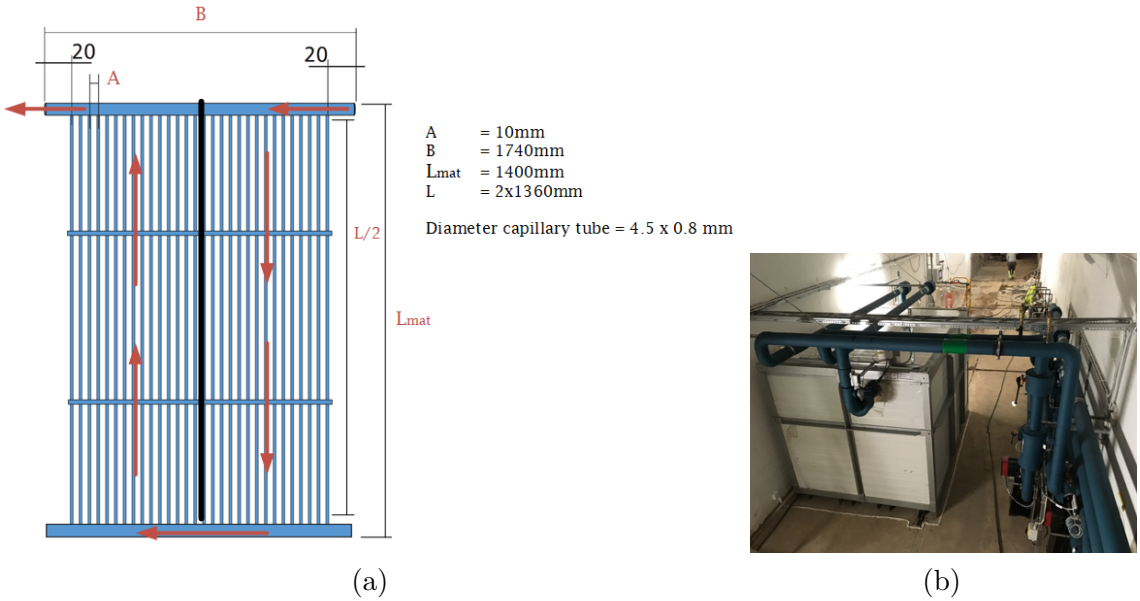

(a) (b)

Figure 4.1: Sketch of capillary tube mat and flow distribution used in the full scale storage (a). Photo of PCM TES installation located in the lower floor (b). Taken from **Paper 4**.

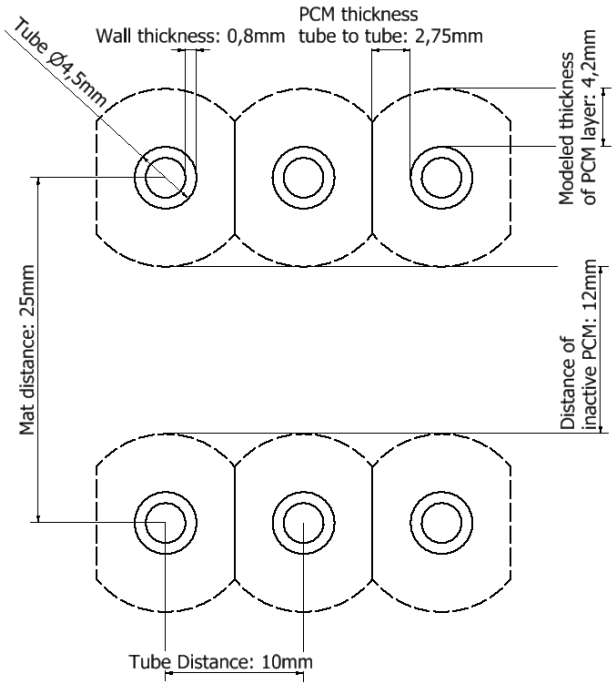

Figure 4.2: Two-dimensional sketch of capillary tube and mat arrangements in the storage (Top View). Taken from **Paper 4**.

4.2.1 Process description

The PCM TES is connected to the campus district cooling and air handling unit (AHU) system of the building according to Fig. 4.3. Water is used as heat transfer fluid in the whole system. Charging the storage occurs via the heat exchanger VVX1 and the storage inlet temperature (sensor GT43) is kept at a setpoint of approximately 8 °C. Discharging occurs via VVX2. During the test period in **Paper 4**, the storage inlet temperature during discharging was typically between 14-16 °C. The cold storage outlet temperature (GT12) is used to pre-cool the main return line of the AHU system at KB01-GT12. During storage discharging, the main cooling load that the district cooling system delivers to the AHU system at KB01-VVX1 is then reduced. Discharging stops when the storage outlet cutoff temperature reaches 14 °C. Tab. 4.2 presents the temperatures of the system and a complete functional description is given in **Paper 4**. Compared to the laboratory study of **Paper 3**, the AHU return temperature was 2 °C lower than initially planned, which leads to a maximum storage temperature difference of 8 instead of 10 °C during the test period.

The heat exchangers VVX1 and VVX2 also have the safety function in the event of a PCM leakage to prevent a contamination of the remaining systems.

Table 4.2: Overview of nominal system operation temperatures with respect to Fig. 4.3 (from **Paper 4**).

Sensor	Description	Value
KB01-GT11	Supply temperature AHU	12 °C
KB01-GT51 & GT48	Return temperature AHU	16 °C
GT41	Supply temperature District Cooling	6-8 °C
GT42	Return temperature District Cooling	16-8 °C
GT43	Inlet temperature TES (T_{in})	Charging: 8 °C Discharging: 14-16 °C
GT12	Outlet temperature TES (T_{out})	Charging: 16-8 °C Discharging: 8-16 °C

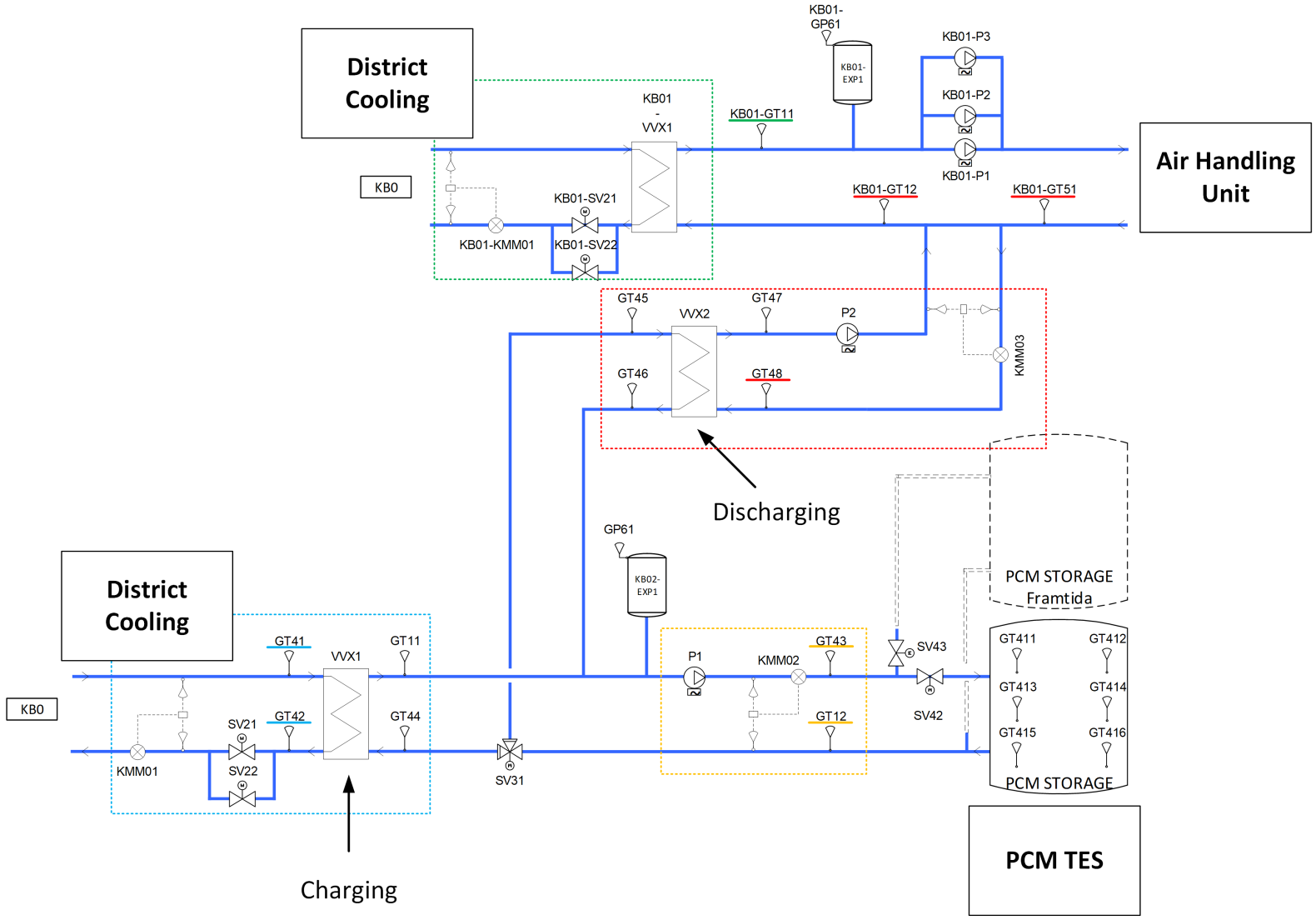

Figure 4.3: System Overview (from **Paper 4**). Important areas are color marked for readability: Main district cooling connection (green box); District cooling connection for charging PCM TES (blue box); Connection between AHU and PCM TES for discharging (red box); Pump and energy meter of PCM TES (yellow box).

4.2.2 Storage benchmarking

First testing was performed during summer 2019 on days when there was cooling load from the air handling unit. During the test period, three pump speed settings were used to charge/discharge the storage with a constant HTF flow rate. The storage was discharged using low (Case C), medium (Case B) and high (Case A) flow rates (4.3). On the other hand, charging was always performed with the highest available flow rate (Case A) of pump P1 in order to decrease charging times as much as possible. The results showed a good repeatability indicating that the SAP mixed with the PCM successfully prevented severe phase separation (Fig. 4.4) during this test phase compared to the laboratory storage. The tests showed that the design intend of decreasing the main district cooling load $P_{KB01-KMM01}$ can be achieved upon discharging the storage (Fig. 4.5).

However, it was found that the storage exhibited significant lower charging power and storage capacity than specified by the manufacturer. For a daily storage, the charging time may not exceed 14-18 hours. During this duration only 36 % of the theoretical installed capacity can be charged to the storage. The useful capacity is thus determined to be $Q_{TES} = 99\,\text{kWh}$ (Fig. 4.6). This capacity can be discharged within 5 hours from the storage with the storage outlet temperature remaining below the cutoff temperature (Fig. 4.5). The average charging and discharging power were estimated to be $\bar{P}^{ch}_{TES} = 7.1 - 5.5\,\text{kW}$ and $\bar{P}^{dch}_{TES} = 19.8\,\text{kW}$, respectively.

Table 4.3: Measured flow rates for different pump speed settings (from **Paper 4**). During charging, pump 1 was always set to "A: High". For discharging, pump 1 was varied according to the cases A, B and C. The highest setting was always chosen during discharging for pump 2.

Case	Pump 1	Pump 2
C: Low	4300-4400L h^{-1}	-
B: Medium	5300-5400L h^{-1}	-
A: High	6800-6900L h^{-1}	4700-4800L h^{-1}

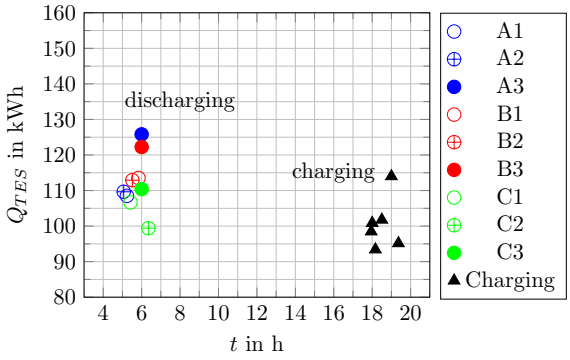

Figure 4.4: Measured discharging and charging capacities during June-August 2019 (from **Paper 4**).

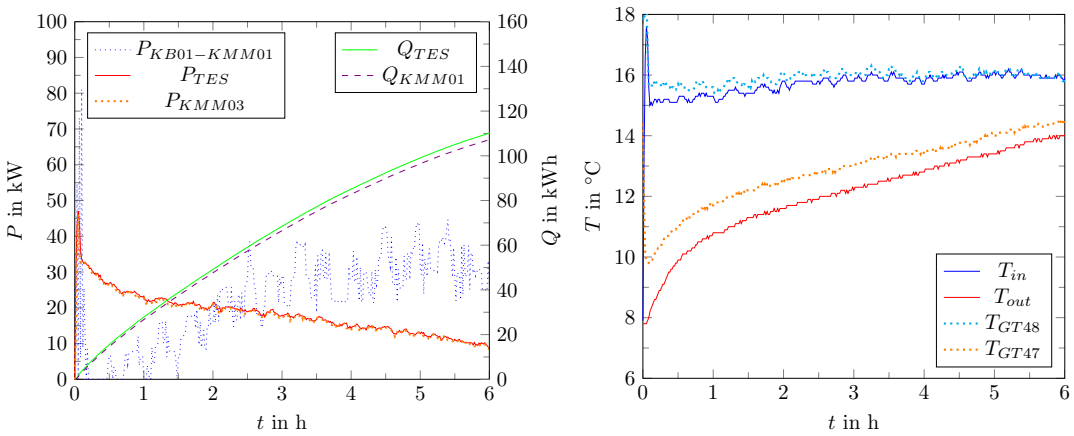

(a) Power and capacity (b) HTF temperatures

Figure 4.5: Example of PCM TES discharging (Case C3). In (a), the red solid and dotted lines are overlapping. Taken from **Paper 4**.

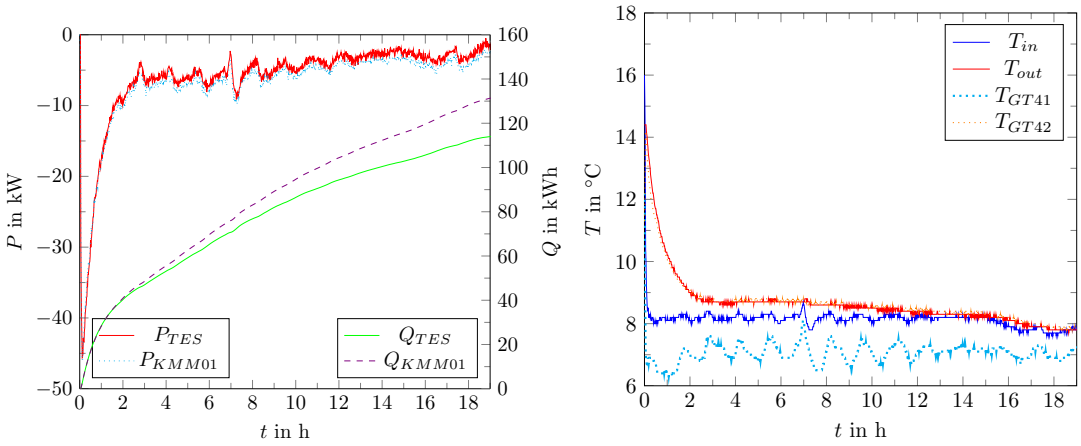

(a) Power and Capacity (b) HTF temperatures

Figure 4.6: Example of PCM TES charging (Case C3). Taken from **Paper 4**.

The useful storage density with respect to the external storage volume is thus $\delta_{tot}^{TES} = 8.84\,\mathrm{kW\,h\,m^{-3}}$ (see Fig. 4.7). This large discrepancy compared to the measured material storage density $\delta_{PCM}^{0} = 46.33\,\mathrm{kW\,h\,m^{-3}}$ on a T-History sample is caused by a large amount of inactive PCM in the storage.

The PCM TES was delivered with six internal PT100 temperature sensors. These sensors are distributed over the height of the storage in the space between two capillary tube mats. It was decided to not include the readings of these sensors in **Paper 4**, as it is currently not clear how to interpret their readings. Fig. 4.8 shows the in/outlet temperature of the storage together with the internal temperature readings for the charging and discharging case C3. Over the course of charging, all internal sensors indicate temperatures not lower than 10.5-11.0 °C, while the outlet temperature of the storage becomes equal to the inlet temperature of ca. 8.0 °C. Control measurements through a small opening on top of the storage via a calibrated

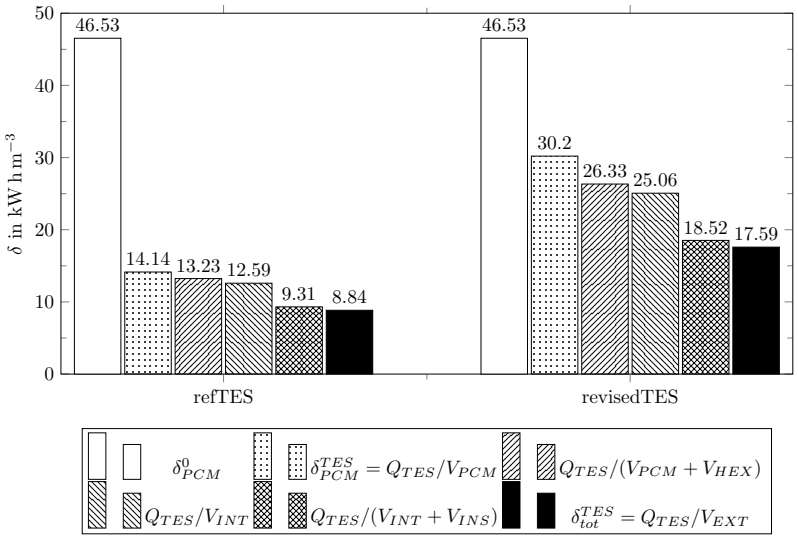

Figure 4.7: Comparison of storage density δ_i (kW h m^{-3}) for different reference volumes (from **Paper 4**). refTES denotes the actual measured storage performance. The revised design are estimates based on an increased density of capillary tubes in the PCM TES.

PT100 sensor (±0.2 °C accuracy) were conducted at the end of charging. The control measurements displayed temperatures in the range of 8.5-9.9 °C which were 1.1-2.0 °C lower than the internal sensor readings. On the other hand during discharging, the internal sensors indicate temperatures higher than the inlet temperature, which should not be physically possible. At the time of writing this thesis, the storage owner is in contact with the storage manufacturer in order to find possible reasons behind the apparent systematic bias towards higher temperatures for the internal sensors and the lower than expected storage capacity.

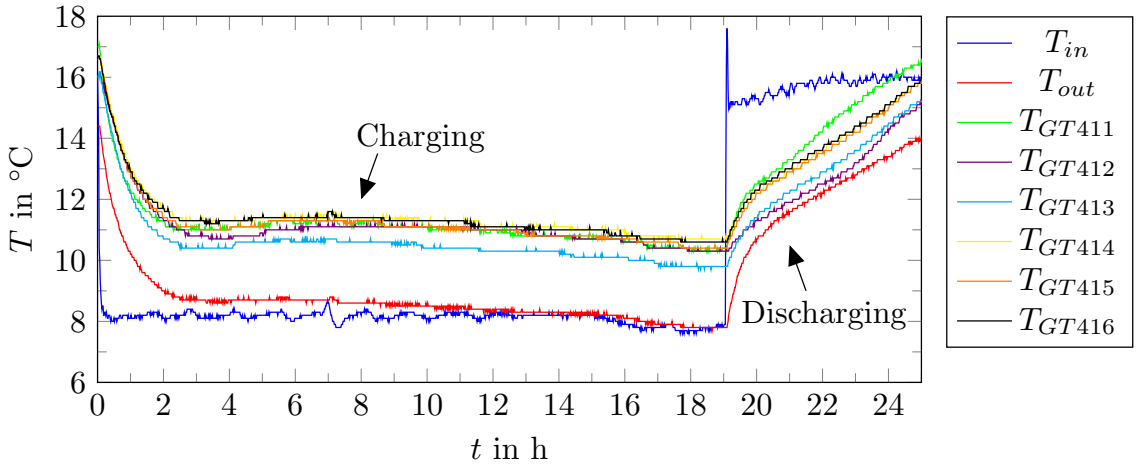

Figure 4.8: Recorded temperature measurements from the internal tank sensors $GT411$ to $GT416$ for charging and discharging of case C3.

4.2.3 Numerical model

A finite volume method (FVM) model was used in order to asses the measured storage performance. The model is based on an energy balance equation and assumes a prescribed and fully developed velocity profile for the HTF. For the PCM domain, only heat conduction is considered (Fig. 4.9). Latent heat is included via the source term method by Voller [113]. The model and its parameters are described in more detail in **Paper 4** and in an earlier licentiate thesis [76]. It has been tested for consistency of temporal and mesh discretization in [76].

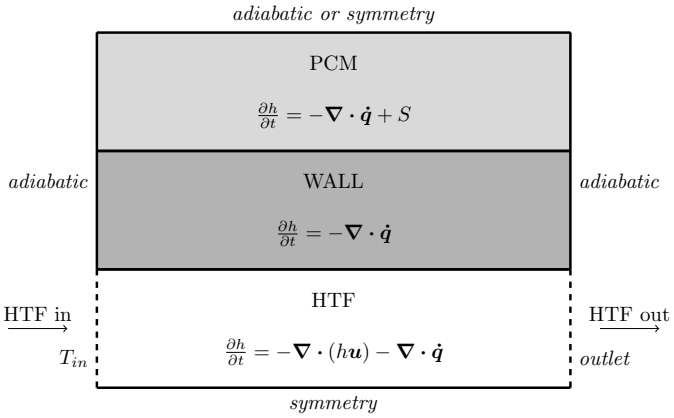

Figure 4.9: Overview of balance equations and boundary conditions for the simulated two-dimensional domain (axial view). Taken from **Paper 4**.

It is estimated that only a thin PCM layer around a single capillary tube is actively storing latent heat (see modeled PCM layer in Fig. 4.2). Since temperature information from within the tank was not reliable, an adiabatic boundary was assumed for the PCM layer. This is a serious simplification as it neglects the sensible storage capacity of the rest of the domain. It is clear that this needs to be re-evaluated when both the actual temperature field of the storage can be measured and the reasons behind the storage performance has been determined. Nevertheless, the model results show an acceptable agreement with all discharging results (Fig. 4.10).

The same model can not be used for charging (Fig. 4.11) and more work is needed to explain the low charging rates of the storage. Fig. 4.12 shows a comparison of the measured T-History curves of two SP11 samples that were taken from the same batch. One of the samples was mixed together with 3 w-% of the SAP and shows a noticeably different solidification curve. It appears that solidification is delayed with a lowered supercooling temperature of ca. 9.0 °C compared to 9.7 °C for the original SP11 sample. Therefore, the effect of SAP on supercooling and the solidification rate of SP11 should be further investigated. If the liquid PCM solution is absorbed by the superabsorbent polymer, it is possible that the transition of the water molecules back into the salt crystal lattices upon solidification is affected:

$$\underbrace{AB(aq) + H_2O(l)}_{\text{absorbed}} \xrightarrow{Solidification} AB \cdot H_2O(s) \tag{4.1}$$

In this case, sorption kinetics may have to be included in the mathematical model.

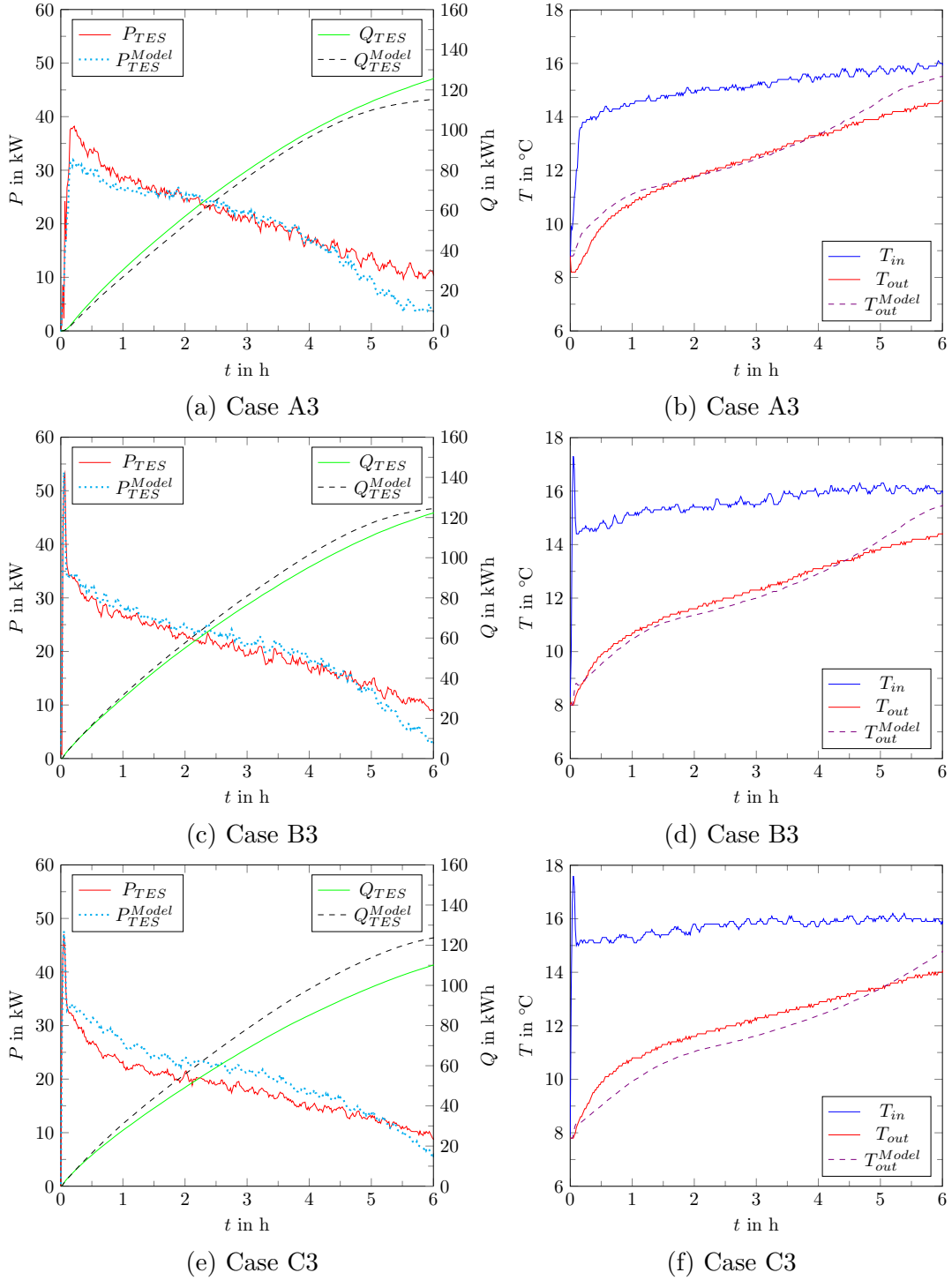

(a) Case A3 (b) Case A3

(c) Case B3 (d) Case B3

(e) Case C3 (f) Case C3

Figure 4.10: Simulation results for discharging cases (from **Paper 4**).

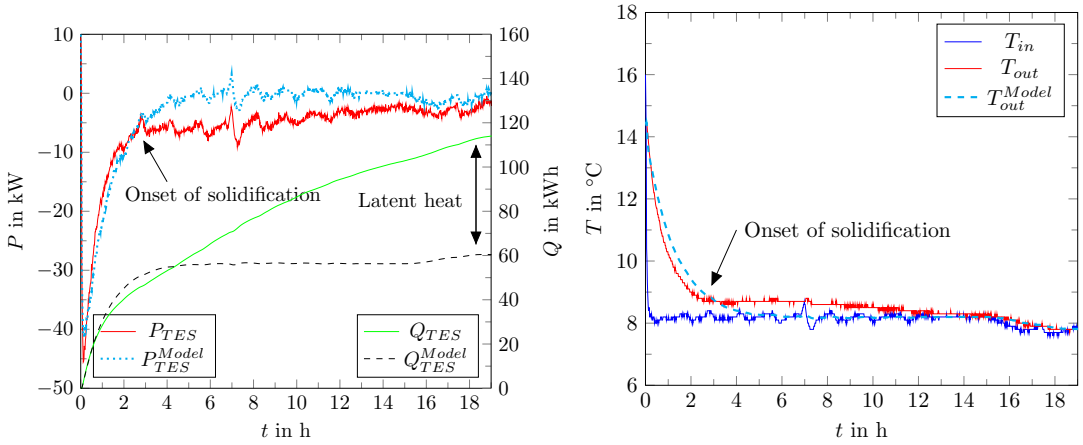

(a) (b)

Figure 4.11: Model results for charging with latent heat set to zero ($L_{PCM} := 0\,\mathrm{kJ\,kg^{-1}}$). Taken from **Paper 4**.

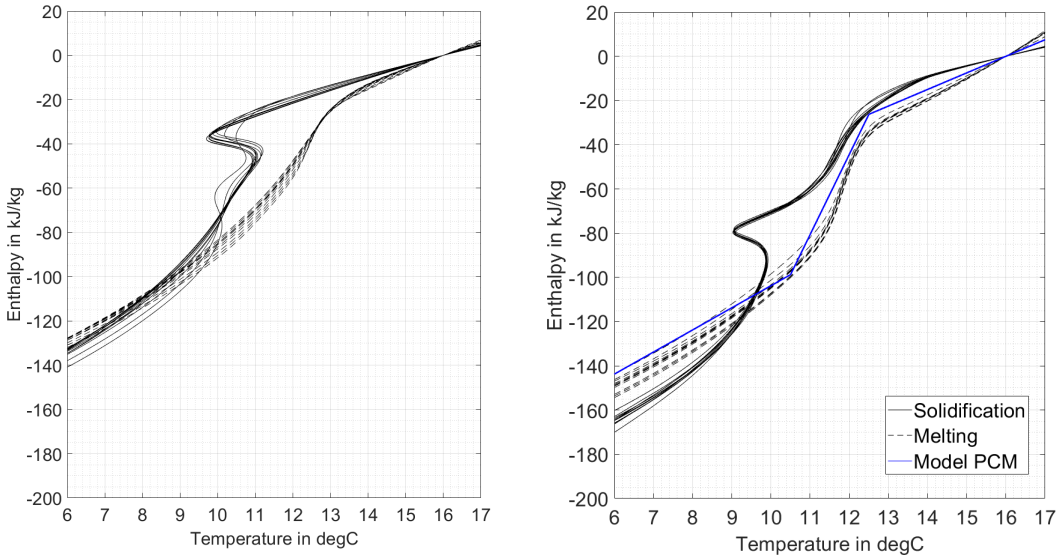

(a) SP11 (b) SP11 with 3 wt-% FAVOR PAC

Figure 4.12: Enthalpy versus temperature curves for two SP11 samples from the same batch (original PCM (a), with added superabsorbent polymer (SAP) (b), 11 T-History cycles). Normalization of enthalpy values at 16 °C. Taken from **Paper 4**.

4.2.4 Economic analysis

The measured performance of the previous sections are used as input parameters in a mixed linear integer programming (MILP) optimization model in order to estimate the economic boundaries of the case study (Fig. 4.13). The model formulation can be found in detail in **Paper 4**. The model uses as input a cooling load simulation of the office building over a representative year (hourly resolution) and determines for each day over the year at which time the PCM TES should be discharged in order to minimize the total annual energy costs. In the studied case, the storage operator reduces these costs by profiting from lower energy prices between charging/discharging and from reducing an additional surcharge based on the monthly peak power consumption.

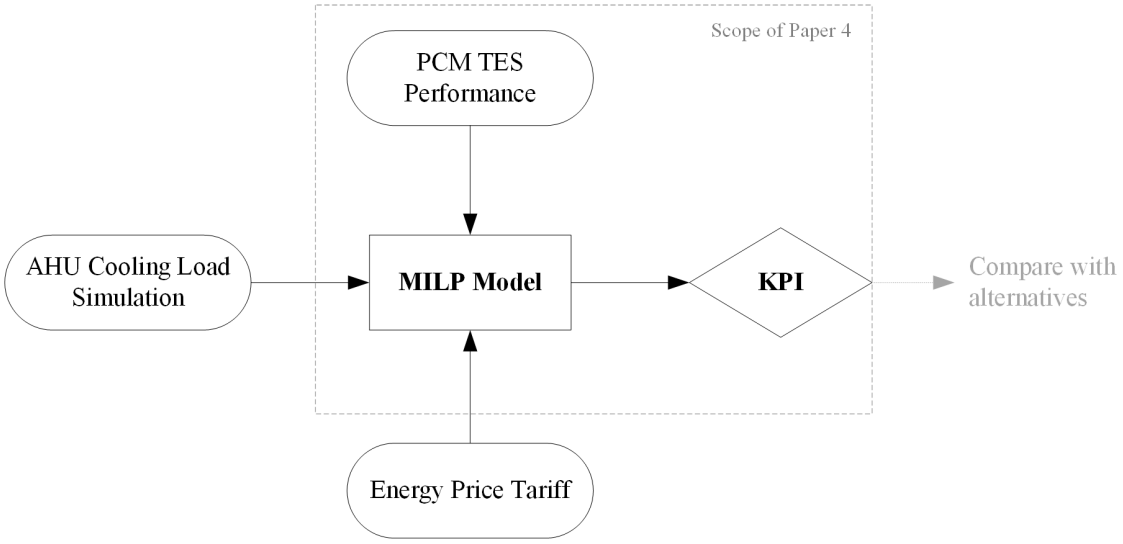

Figure 4.13: Flowchart for calculating economic KPI.

In **Paper 4**, different variations of the measured PCM TES performance (Case '$refTES$') are evaluated in the model (see table 4.4). The cases '$refTESnoETA$' and '$refTESnoAux$' study the reference case without thermal cycling losses and with negligible operating costs of the pumps during charging and discharging, respectively. The case '$revisedTES$' assumes a better storage performance when the capillary tube density in the storage is increased. Moreover, two additional cases '$refTES2x$' and '$revisedTES2x$' are studied, which both consider two independently dischargeable storages. These last two cases are included because the option to install a second storage into the system via valve SV43 (Fig. 4.3) is available for the future.

Fig. 4.14 shows the duration curves for the AHU cooling load that has to be covered by the district cooling network. It can be seen that the peak power consumption can be decreased noticeably for all cases. From the curve, it can also be seen that a single storage is not able to reduce the district cooling load after the initial peak reduction. This is because the simulated building cooling load consists of a longer duration than the five hours of storage discharge time. This limitation of storage capacity is visible when the duration curve of the cases with storage

Table 4.4: Studied cases of the MILP model (from **Paper 4**).

Case	Description
noTES	Business as usual without TES
refTES	Current TES design
refTESnoETA	Current TES design, no cycling losses
refTESnoAux	Current TES design, no auxiliary equipment costs
revisedTES	Revised TES design
refTES2x	2x Current TES design
revisedTES2x	2x Revised TES design

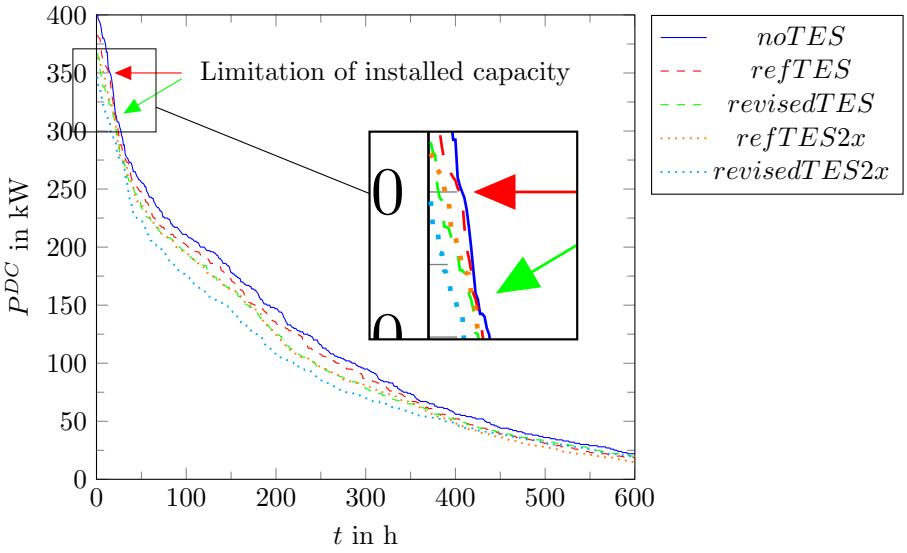

Figure 4.14: Duration curve of P^{DC} for the business as usual case $noTES$ and the optimum solution of cases $refTES$, $revisedTES$, $refTES2x$ and $revisedTEX2x$ (from **Paper 4**).

matches the original duration curve without storage. The added benefit of a second storage can be seen in Fig. 4.15, where the optimum solution would be to discharge the second storage with a two hour delay in order to yield the lowest peak power consumption on the most critical day in July.

The economic benefits of all studied cases are summarized in Tab. 4.5. The main cost savings for this application stem from the reduction of the peak power consumption surcharge. The reduction of energy consumption costs on the other hand is small due to two reasons: 1) a relatively low energy price difference during charging and discharging and 2) because of the additional energy cost due to thermal cycling losses and operating the auxiliary equipment. Under the assumption that these cost reductions occur annually, the investment cost limit for a 5-year payback period can be estimated. This short payback period was chosen as it reflects typical industry requirements for new investments [114]. Moreover, the storage supplier guaranteed a stable performance of the storage for only five years. This investment

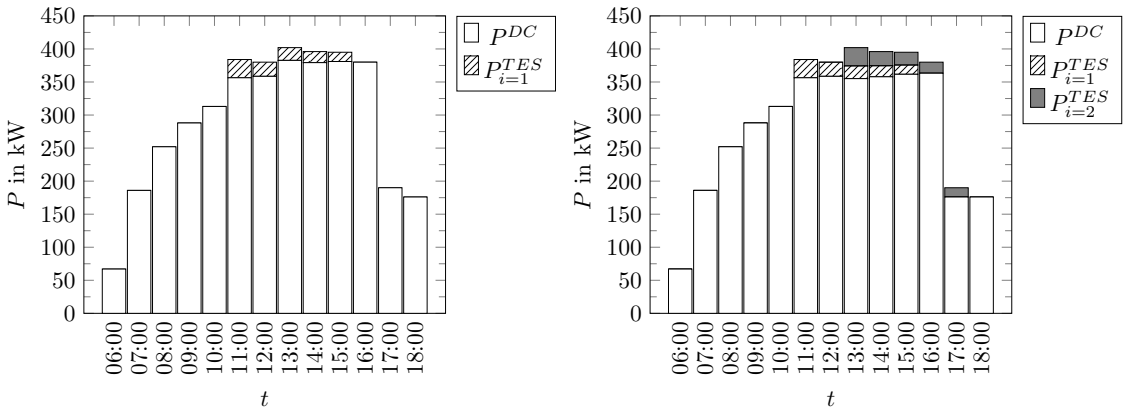

(a) refTES (b) refTES2x

Figure 4.15: Examples of optimum solutions for the most critical day of the month: July 31st (from **Paper 4**).

cost limit is listed as the economic key performance indicator in **Paper 4** and can be compared to other storage designs for this application. Longer payback periods can be considered if information on the expected lifetime and maintenance costs of the storage is available. Then a more thorough life cycle cost (LCC) analysis should be done. For the studied case, the actual storage investment costs were 546 452 SEK (51 350 EUR). Thus, the storage costs have to be significantly decreased in order to yield acceptable payback times.

Table 4.5: Overview of annual cost reductions from case *noTES* and the maximum allowed investment costs for the PCM TES with a payback time of five years (from **Paper 4**). Currency conversion rate used: 10.65 SEK/EUR

Case	Cost reduction: Power (%)	Cost reduction: Energy (%)	Cost reduction: Total (%)	Investment cost limit (SEK/EUR)
refTES	-8.19	-0.76	-4.17	9804 / 921
refTESnoETA	-8.19	-1.16	-4.38	10303 / 967
refTESnoAux	-8.19	-3.60	-5.71	13425 / 1261
revisedTES	-13.03	-1.08	-6.55	15421 / 1448
refTES2x	-15.10	-1.42	-7.68	18076 / 1697
revisedTES2x	-22.84	-2.06	-11.58	27235 / 2557

It should be noted that the methodology in Fig. 4.13 can be already used in early stages of a PCM TES project. The storage can be essentially seen as a black box, where only the parameters of the storage HTF during charging and discharging are relevant. Different combinations of power/capacity ratios can be used as input parameters and their costs and benefit ratio estimated. This is necessary as the present energy tariff favors peak power reduction as the main economic incentive for TES. Moreover, also data from other TES technologies such as the discharge curves of a sensible water storage can be used, which makes comparison across different TES types possible. While the model assumed optimum control, the result should

be compared against simple rule based controls as well. The assumption of perfect cooling load forecast should also be checked against the actual cooling demand in the future.

4.3 Conclusions & outlook

A full scale PCM TES installation is studied in **Paper 4**. Key performance indicators are systematically determined for the storage through repeated measurements. It was found that only about 99 kWh from the manufacturer value of 275 kWh can be utilized in daily operation. The charging time was determined to be the limiting factor for utilizing more storage capacity. Future work needs to be done in order to explain the low charging rates. While the addition of sodium polyacrylate as superabsorbent polymer into the PCM prevented phase-separation, its effect on supercooling and solidification of the PCM should be studied. PCM samples from different storage locations have to be accessed and analyzed. Using a simple numerical model to fit the experimental data, it appears that only a thin layer of PCM around each capillary tube stores latent heat. The storage needs to be retrofitted with working temperature sensors to provide more accurate model predictions. The model should then be extended to a 3-D model to take into account the pitch offset of the capillary tubes between two mats in the existing storage. The model also needs to be verified for both charging and discharging.

The economic performance of the storage was estimated based on its technical performance. In this work, it is represented by the allowed investment cost limit based on a five year payback time. The proposed methodology is general and can be used to study other design alternatives. It also allows to investigate the economic boundaries and trade-offs for different design decisions. For example, the costs of improving discharge rates through the increase of heat exchanger area in the storage can be related to the resulting economic benefit.

For future work, a methodology should be developed that combines optimum storage sizing and control in order to maximize the economic benefits. Since optimum scheduling is assumed, more work needs to be done on how to implement the storage control system in practice. An accurate building and campus-wide cooling load prediction may be necessary to determine the optimum time to discharge the storage in order to reduce the peak cooling load for the complete campus. In addition, it should be compared against simpler rule-based strategies.

It is pointed out that economic KPI's are usually case dependent and need to be re-evaluated depending on the boundary conditions of the application. Therefore, work should focus on finding scenarios where a PCM TES is an economically viable storage choice. Compared to sensible storages, it may be necessary that a potentially high storage density can be translated to an additional economic benefit, such as floor space savings. A PCM TES may also be more economically viable compared to a purchase of a new cooling machine in certain situations. For a proper evaluation, a more accurate LCC analysis needs to be performed. Then more information regarding lifetime and maintenance costs of PCM TES needs to be available.

Chapter 5

Final conclusions

In this thesis, the design of a PCM TES is comprehensively studied and revealed certain limitations of current design approaches on material, device and system scale. The work provides more insights on how these can be improved.

On material scale, the accuracy of enthalpy curves for PCMs determined from T-History setups with insulated sample holders is studied numerically and experimentally. It is shown in **Paper 1** and **2** that the present insulation leads to systematic errors in the resulting enthalpy-temperature curve and that the data evaluation method needs to be adjusted in order to yield repeatable results. The obtained values using T-History can only be seen as approximations, since it was shown that the results can be sensitive to both the experimental conditions and the performed data evaluation method. Therefore, the T-History method needs a standardization within both aspects. From the work of the two papers, however, the experimental setup can be chosen depending on the priority of the user, while being aware of the trade-offs. As an example, if the accurate determination of the phase change temperature range is the priority, then it may be still feasible to increase the insulation thickness in order to decrease the artificial hysteresis.

On device scale, the capacity effectiveness during consecutive charging and discharging cycles was studied on a laboratory prototype of the chosen PCM TES under reproduced process conditions. It is shown in **Paper 3** that the useful storage capacity/density is significantly reduced already after the first (dis-)charging cycle compared to the manufacturer estimate. By performing T-History measurements on samples taken at different heights in the storage before and after cycling, it was possible to show that the salt-hydrate suffers from phase separation and increased supercooling. Interestingly, T-History of these isolated samples show a stable cycling performance compared to the bulk performance of the material inside the storage. T-History can be used for an initial screening of PCMs in order to evaluate whether the latent heat can be potentially utilized within the process temperatures. However, it may not be a representative testing method to predict the material behavior inside storage prototypes. The selected PCM and heat exchanger/storage geometry need to be taken into account additionally in order to select a representative measurement method. Therefore, prototyping on device scale is recommended whenever possible.

This way the additional risks of phase separation and supercooling of the materials under process conditions can be evaluated.

As a result from the observations on device scale, a superabsorbent polymer was added to the salt-hydrate to prevent phase separation in the full scale storage by the storage supplier. This installation is presented and studied in **Paper 4**. Repeated measurements showed that only 36 % of the manufacturer estimate for the installed storage capacity can be effectively charged and discharged (within 14-18 h and 5 h, respectively) in daily operation. The storage density based on the external storage volume is then 8.84 kW h m^{-3} compared to a measured theoretical possible material storage density of 46.53 kW h m^{-3} using T-History. The useful storage capacity is limited due to lower charging rates than expected. This low performance shows that there is still a knowledge gap in designing PCM TES with commercial PCMs. A reason for the performance deviation may be the effect of the SAP on solidification of the salt-hydrate, but this has to be investigated further. A simplified simulation model indicates that a large part of the PCM appears to be inactive in storing latent heat.

An economic analysis was then conducted using the measured technical performance of the storage and a cooling demand simulation of the office building over a year. It is shown that for the local energy price tariff, the major cost benefit of operating the storage stems from reducing the monthly power consumption fee of the utility company. It is also shown that an increase of the storage discharge power and a higher installed capacity (leading to longer discharge durations of up to seven or eight hours) would yield higher yearly energy cost savings. Based on these economic benefits, an storage investment cost limit can be defined as KPI that would allow a five year payback time. In this case study, it was found that the actual investment costs exceeded this limit. While an optimum scheduling is assumed, the methodology can still be used to estimate the economic feasibility of different TES design options. This simple economic analysis could be performed at early design stages for different power to capacity ratios. However, reliable models predicting the PCM TES performance and/or prototype measurement data, which can be upscaled, need to be available in practice. Furthermore, reliable information of the PCM TES lifetime are needed to perform a more detailed life cycle cost analysis.

It can be concluded that designing a fully functional PCM TES using commercial salt-hydrates at low cost is still a challenging task. In the case study, the available process temperature difference for charging and discharging the storage is narrow so that the storage performance becomes sensitive to unexpected and unfavorable material properties. Which is why material testing becomes even more important. It is likely that more room for errors and uncertainties in the PCM TES design are available for heat storage applications due to typically wider process temperature differences. However, in these cases available sensible TES technologies such as water storages become also more favorable, since the storage capacity/density of sensible TES increases.

Chapter 6

Outlook & future work

More work needs to be done in order to find economically acceptable applications and scenarios for PCM TES. At the same time, the investment cost limits for potential storage applications should be determined. These can serve as guidance to prioritize future research. It may be more practical to follow a top down approach of the material/device/system scales outlined in Section 1.2.

Different processes and energy price tariffs can be first analyzed regarding which theoretical storage charging/discharging power to capacity ratio is optimal for the process. This can be based on economic or ecological benefits of the storage. Thus, this stage provides the information which application of the TES is feasible for the process. A daily storage for peak shaving typically favors a high power to capacity ratio, while a seasonal storage likely prioritizes capacity over charging/discharging power [115]. It is also necessary to consider that different control strategies for the same storage may lead to different benefits. Thus, it should be studied how sensitive the resulting storage benefits are with respect to simple rule-based or more advanced control strategies. Moreover, thermal losses should be quantified as a decrease of the storage's economic and ecological benefits.

This way potential applications and economic boundaries can be found for which a thermal energy storage is an acceptable investment decision. It should be noted that the outcome also depends on individual scenarios of the same process. For the case study, a significant additional argument towards a storage would have been given in a scenario when the installed capacity of the cold energy generation units can be simultaneously decreased. The search for the ideal installed storage power and capacity should be performed in general terms from which then a storage technology is selected. A PCM TES may be more competitive than sensible storages, when a smaller storage size or the release of latent heat at a constant temperature has an economic value or is a requirement.

On device scale, the task would then be to utilize as much of the theoretical PCM storage capacity as possible based on the specified power and capacity. This is again a trade-off and optimization task. On one hand, the heat transfer area between the HTF and PCM has to be large enough so that the power and capacity demand is reached. On the other hand, a larger heat exchanger increases the storage

volume (and decreases the overall storage density) and leads to higher material costs. However, if the heat exchanger area is not sufficient, the actual cost of the storage material increases, since a larger fraction of the storage material can not be utilized in the process. This is an optimization task depending on process temperatures, HTF flow rates and material thermal properties as shown via simulations by Fang [50, 69] and in the prior licentiate thesis [76]. For the presented case study in this thesis, it should be investigated whether the heat exchanger geometry can be further optimized. However, accurate PCM models need to be available as input data.

When performing the design task, it is important to consider that the storage remains economically (and ecologically) feasible with respect to the acceptable storage costs from the system analysis. It should also be determined how much insulation is to be applied so that the additional investment cost of the insulation material is accounted for by reducing the thermal losses during storage operation. The costs of the PCM TES should be compared to existing reference technologies, such as sensible water storages, in order to select the best storage technology for the application.

On material scale, more work needs to be done to determine accurate and representative material properties. The need for a PCM database for the design process has already been stated in Lane 1983 [26], but standardization of PCM test methods need to be first established. More detailed recommendations for applying which of the available characterization methods should be developed. This can be based on how accurately they predict the material behavior within the storage depending on the chosen PCM and the given heat exchanger design.

In general, material prices have to be decreased for available PCMs and a certain lifetime of the material should be guaranteed by suppliers. For the case study, salt-hydrates were the cheapest option, but it came with material specific problems like phase separation and supercooling. Moreover, long-term stability is still to be determined for the PCM with the added superabsorbent polymer. The reasons behind the low charging rates of the storage also need to be investigated further. Finding alternative materials by tailoring the phase change temperature for promising applications may be an option. It should also be evaluated if improving storage heat transfer rates should be done by increasing the material thermal conductivity or via larger heat transfer areas in the storage device. The cost to benefit ratio of each measure then needs to be compared.

Such a top down approach can be seen as necessary, because there are currently little commercial PCM TES available that can be considered for a potential storage application. This way, research effort on material and device scale can be focused on the most suitable applications first.

References

[1] International Energy Agency. *Energy Technology Perspectives 2017*. ISBN: 978-92-64-27597-3 (cit. on p. 3).

[2] Gadd, H. and Werner, S. "Thermal energy storage systems for district heating and cooling". In: *Advances in Thermal Energy Storage Systems* (2015), pp. 467–478. DOI: 10.1533/9781782420965.4.467 (cit. on p. 3).

[3] Heier, J. et al. "Combining thermal energy storage with buildings – a review". In: *Renewable and Sustainable Energy Reviews* 42 (2015), pp. 1305–1325. DOI: 10.1016/J.RSER.2014.11.031 (cit. on pp. 3, 43).

[4] Navarro, L. et al. "Thermal energy storage in building integrated thermal systems: A review. Part 2. Integration as passive system". In: *Renewable Energy* 85 (2016), pp. 1334–1356. DOI: 10.1016/j.renene.2015.06.064 (cit. on pp. 3, 6).

[5] Aneke, M. and Wang, M. "Energy storage technologies and real life applications – A state of the art review". In: *Applied Energy* 179 (2016), pp. 350–377. DOI: 10.1016/j.apenergy.2016.06.097 (cit. on pp. 3, 4, 6).

[6] Yau, Y. H. and Rismanchi, B. "A review on cool thermal storage technologies and operating strategies". In: *Renewable and Sustainable Energy Reviews* 16.1 (2012), pp. 787–797. DOI: 10.1016/j.rser.2011.09.004 (cit. on pp. 3, 9, 10).

[7] Sun, Y. et al. "Peak load shifting control using different cold thermal energy storage facilities in commercial buildings: A review". In: *Energy Conversion and Management* 71 (2013), pp. 101–114. DOI: 10.1016/j.enconman.2013.03.026 (cit. on pp. 3, 9, 10).

[8] Ooka, R. and Ikeda, S. "A review on optimization techniques for active thermal energy storage control". In: *Energy and Buildings* 106 (2015), pp. 225–233. DOI: 10.1016/J.ENBUILD.2015.07.031 (cit. on pp. 3, 9, 10).

[9] Odufuwa, O. Y. et al. "Review of Optimal Energy Management Applied on Ice Thermal Energy Storage for an Air Conditioning System in Commercial Buildings". In: *Proceedings in Open Innovations Conference*. IEEE, 2018, pp. 285–292. ISBN: 9781538653166. DOI: 10.1109/OI.2018.8535839 (cit. on pp. 3, 9, 10).

[10] Kousksou, T. et al. “Energy storage: Applications and challenges”. In: *Solar Energy Materials and Solar Cells* 120 (2014), pp. 59–80. DOI: 10.1016/j.solmat.2013.08.015 (cit. on p. 3).

[11] Zalba, B. et al. “Review on thermal energy storage with phase change: materials, heat transfer analysis and applications”. In: *Applied Thermal Engineering* 23.3 (2003), pp. 251–283. DOI: 10.1016/S1359-4311(02)00192-8 (cit. on pp. 3, 4, 6, 8, 10).

[12] Mehling, H. and Cabeza, L. F. *Heat and cold storage with PCM: An up to date introduction into basics and applications; with 28 tables*. Heat and Mass Transfer. Springer, 2008. ISBN: 354068557X (cit. on pp. 3, 4, 6, 8, 10, 17, 19, 33, 34, 42).

[13] Cabeza, L. F. et al. “Materials used as PCM in thermal energy storage in buildings: A review”. In: *Renewable and Sustainable Energy Reviews* 15.3 (2011), pp. 1675–1695. DOI: 10.1016/j.rser.2010.11.018 (cit. on pp. 3, 4, 6, 8, 10).

[14] Hyun, D. C. et al. “Emerging applications of phase-change materials (PCMs): Teaching an old dog new tricks”. In: *Angewandte Chemie (International ed. in English)* 53.15 (2014), pp. 3780–3795. DOI: 10.1002/anie.201305201 (cit. on pp. 3, 6, 8, 10).

[15] Lizana, J. et al. “Identification of best available thermal energy storage compounds for low-to-moderate temperature storage applications in buildings”. In: *Materiales de Construcción* 68.331 (2018), p. 160. DOI: 10.3989/mc.2018.10517 (cit. on pp. 3, 6, 8, 10).

[16] Nazir, H. et al. “Recent developments in phase change materials for energy storage applications: A review”. In: *International Journal of Heat and Mass Transfer* 129 (2019), pp. 491–523. DOI: 10.1016/j.ijheatmasstransfer.2018.09.126 (cit. on pp. 3, 4, 6, 8, 10, 43).

[17] Rismanchi, B. et al. “Energy, exergy and environmental analysis of cold thermal energy storage (CTES) systems”. In: *Renewable and Sustainable Energy Reviews* 16.8 (2012), pp. 5741–5746. DOI: 10.1016/j.rser.2012.06.002 (cit. on p. 4).

[18] Arteconi, A. et al. “State of the art of thermal storage for demand-side management”. In: *Applied Energy* 93 (2012), pp. 371–389. DOI: 10.1016/j.apenergy.2011.12.045 (cit. on p. 4).

[19] Oró, E. et al. “Review on phase change materials (PCMs) for cold thermal energy storage applications”. In: *Applied Energy* 99 (2012), pp. 513–533. DOI: 10.1016/j.apenergy.2012.03.058 (cit. on p. 4).

[20] Gracia, A. de and Cabeza, L. F. “Phase change materials and thermal energy storage for buildings”. In: *Energy and Buildings* 103 (2015), pp. 414–419. DOI: 10.1016/J.ENBUILD.2015.06.007 (cit. on p. 4).

[21] Kalnæs, S. E. and Jelle, B. P. "Phase change materials and products for building applications: A state-of-the-art review and future research opportunities". In: *Energy and Buildings* 94 (2015), pp. 150–176. DOI: 10.1016/j.enbuild.2015.02.023 (cit. on p. 4).

[22] Li, S.-F. et al. "A comprehensive review on positive cold energy storage technologies and applications in air conditioning with phase change materials". In: *Applied Energy* 255 (2019), p. 113667. DOI: 10.1016/j.apenergy.2019.113667 (cit. on pp. 4, 43).

[23] Agyenim, F. B. et al. "A review of materials, heat transfer and phase change problem formulation for latent heat thermal energy storage systems (LHTESS)". In: *Renewable and Sustainable Energy Reviews* 14.2 (2010), pp. 615–628. DOI: 10.1016/j.rser.2009.10.015 (cit. on p. 4).

[24] Pereira da Cunha, J. and Eames, P. "Thermal energy storage for low and medium temperature applications using phase change materials – A review". In: *Applied Energy* 177 (2016), pp. 227–238. DOI: 10.1016/j.apenergy.2016.05.097 (cit. on p. 4).

[25] Kenisarin, M. and Mahkamov, K. "Passive thermal control in residential buildings using phase change materials". In: *Renewable and Sustainable Energy Reviews* 55 (2016), pp. 371–398. DOI: 10.1016/J.RSER.2015.10.128 (cit. on p. 4).

[26] Lane, G. A. *Solar Heat Storage: Latent Heat Materials, Vol. I: Background and Scientific Principles*. CRC Press, 1983. ISBN: 9781351076753. DOI: 10.1115/1.3266412 (cit. on pp. 5, 8, 10, 33, 62).

[27] Lane, G. A. *Solar Heat Storage: Latent Heat Materials, Vol.II: Technology*. CRC Press, 1986. ISBN: 9781351076746 (cit. on pp. 5, 8, 10, 33).

[28] Navarro, L. et al. "Thermal energy storage in building integrated thermal systems: A review. Part 1. active storage systems". In: *Renewable Energy* 88 (2016), pp. 526–547. DOI: 10.1016/j.renene.2015.11.040 (cit. on p. 6).

[29] Song, M. et al. "Review on building energy performance improvement using phase change materials". In: *Energy and Buildings* 158 (2018), pp. 776–793. DOI: 10.1016/j.enbuild.2017.10.066 (cit. on pp. 6, 9, 10).

[30] Akeiber, H. et al. "A review on phase change material (PCM) for sustainable passive cooling in building envelopes". In: *Renewable and Sustainable Energy Reviews* 60 (2016), pp. 1470–1497. DOI: 10.1016/J.RSER.2016.03.036 (cit. on p. 6).

[31] Mavrigiannaki, A. and Ampatzi, E. "Latent heat storage in building elements: A systematic review on properties and contextual performance factors". In: *Renewable and Sustainable Energy Reviews* 60 (2016), pp. 852–866. DOI: 10.1016/J.RSER.2016.01.115 (cit. on p. 6).

[32] Zhu, N. et al. “A review on applications of shape-stabilized phase change materials embedded in building enclosure in recent ten years”. In: *Sustainable Cities and Society* 43 (2018), pp. 251–264. DOI: 10.1016/J.SCS.2018.08.028 (cit. on p. 6).

[33] Chandel, S. S. and Agarwal, T. “Review of current state of research on energy storage, toxicity, health hazards and commercialization of phase changing materials”. In: *Renewable and Sustainable Energy Reviews* 67 (2017), pp. 581–596. DOI: 10.1016/j.rser.2016.09.070 (cit. on pp. 8, 10).

[34] Shukla, A. et al. “Thermal cycling test of few selected inorganic and organic phase change materials”. In: *Renewable Energy* 33.12 (2008), pp. 2606–2614. DOI: 10.1016/j.renene.2008.02.026 (cit. on pp. 8, 10).

[35] Rathod, M. K. and Banerjee, J. “Thermal stability of phase change materials used in latent heat energy storage systems: A review”. In: *Renewable and Sustainable Energy Reviews* 18 (2013), pp. 246–258. DOI: 10.1016/j.rser.2012.10.022 (cit. on pp. 8, 10, 33, 34).

[36] Solé, A. et al. “Stability of sugar alcohols as PCM for thermal energy storage”. In: *Solar Energy Materials and Solar Cells* 126 (2014), pp. 125–134. DOI: 10.1016/j.solmat.2014.03.020 (cit. on pp. 8, 10).

[37] Ferrer, G. et al. “Review on the methodology used in thermal stability characterization of phase change materials”. In: *Renewable and Sustainable Energy Reviews* 50 (2015), pp. 665–685. DOI: 10.1016/j.rser.2015.04.187 (cit. on pp. 8, 10, 32).

[38] Cabeza, L. F. et al. “Immersion corrosion tests on metal-salt hydrate pairs used for latent heat storage in the 48 to 58°C temperature range”. In: *Materials and Corrosion* 53.12 (2002), pp. 902–907. DOI: 10.1002/maco.200290004 (cit. on pp. 8, 10).

[39] Oro, E. et al. “Corrosion of metal and polymer containers for use in PCM cold storage”. In: *Applied Energy* 109 (2013), pp. 449–453. DOI: 10.1016/j.apenergy.2012.10.049 (cit. on pp. 8, 10, 12).

[40] Solé, A. et al. “Corrosion Test of Salt Hydrates and Vessel Metals for Thermochemical Energy Storage”. In: *Energy Procedia* 48 (2014), pp. 431–435. DOI: 10.1016/j.egypro.2014.02.050 (cit. on pp. 8, 10).

[41] Ushak, S. et al. “Compatibility of materials for macroencapsulation of inorganic phase change materials: Experimental corrosion study”. In: *Applied Thermal Engineering* 107 (2016), pp. 410–419. DOI: 10.1016/j.applthermaleng.2016.06.171 (cit. on pp. 8, 10, 12).

[42] Cabeza, L. F. et al. “Unconventional experimental technologies available for phase change materials (PCM) characterization. Part 1. Thermophysical properties”. In: *Renewable and Sustainable Energy Reviews* 43 (2015), pp. 1399–1414. DOI: 10.1016/j.rser.2014.07.191 (cit. on pp. 8, 10, 18, 19, 32).

[43] Inés Fernández, A. et al. "Unconventional experimental technologies used for phase change materials (PCM) characterization: part 2 – morphological and structural characterization, physico-chemical stability and mechanical properties". In: *Renewable and Sustainable Energy Reviews* 43 (2015), pp. 1415–1426. DOI: 10.1016/j.rser.2014.11.051 (cit. on pp. 8, 10, 32).

[44] Solé, A. et al. "Review of the T-history method to determine thermophysical properties of phase change materials (PCM)". In: *Renewable and Sustainable Energy Reviews* 26 (2013), pp. 425–436. DOI: 10.1016/j.rser.2013.05.066 (cit. on pp. 8, 10, 20).

[45] Gschwander, S. et al. "Standardization of PCM Characterization via DSC". In: *Proceedings in Greenstock Conference*. 2015 (cit. on pp. 8, 10, 19, 32).

[46] Gibout, S. et al. "Challenges of the Usual Graphical Methods Used to Characterize Phase Change Materials by Differential Scanning Calorimetry". In: *Applied Sciences* 8.1 (2018), p. 66. DOI: 10.3390/app8010066 (cit. on pp. 8, 10, 18, 19, 32).

[47] Dutil, Y. et al. "A review on phase-change materials: Mathematical modeling and simulations". In: *Renewable and Sustainable Energy Reviews* 15.1 (2011), pp. 112–130. DOI: 10.1016/j.rser.2010.06.011 (cit. on pp. 8, 10).

[48] Klimeš, L. et al. "Computer modelling and experimental investigation of phase change hysteresis of PCMs: The state-of-the-art review". In: *Applied Energy* 263 (2020), p. 114572. DOI: 10.1016/j.apenergy.2020.114572 (cit. on pp. 8, 10, 19).

[49] Castell, A. and Solé, C. "An overview on design methodologies for liquid–solid PCM storage systems". In: *Renewable and Sustainable Energy Reviews* 52 (2015), pp. 289–307. DOI: 10.1016/j.rser.2015.07.119 (cit. on pp. 8, 10).

[50] Fang, Y. et al. "Numerical analysis for maximizing effective energy storage capacity of thermal energy storage systems by enhancing heat transfer in PCM". In: *Energy and Buildings* 160 (2018), pp. 10–18. DOI: 10.1016/j.enbuild.2017.12.006 (cit. on pp. 8, 10, 62).

[51] Ibrahim, N. I. et al. "Heat transfer enhancement of phase change materials for thermal energy storage applications: A critical review". In: *Renewable and Sustainable Energy Reviews* 74 (2017), pp. 26–50. DOI: 10.1016/j.rser.2017.01.169 (cit. on pp. 8, 10).

[52] Rathore, P. K. S. and Shukla, S. K. "Potential of macroencapsulated pcm for thermal energy storage in buildings: A comprehensive review". In: *Construction and Building Materials* 225 (2019), pp. 723–744. DOI: 10.1016/j.conbuildmat.2019.07.221 (cit. on pp. 8, 10).

[53] Lazaro, A. et al. "PCM–air heat exchangers for free-cooling applications in buildings: Experimental results of two real-scale prototypes". In: *Energy Conversion and Management* 50.3 (2009), pp. 439–443. DOI: 10.1016/j.enconman.2008.11.002 (cit. on pp. 8, 10).

[54] Pomianowski, M. et al. “Review of thermal energy storage technologies based on PCM application in buildings”. In: *Energy and Buildings* 67 (2013), pp. 56–69. DOI: 10.1016/j.enbuild.2013.08.006 (cit. on pp. 9, 10).

[55] Alizadeh, M. and Sadrameli, S. M. “Development of free cooling based ventilation technology for buildings: Thermal energy storage (TES) unit, performance enhancement techniques and design considerations – A review”. In: *Renewable and Sustainable Energy Reviews* 58 (2016), pp. 619–645. DOI: 10.1016/j.rser.2015.12.168 (cit. on pp. 9, 10).

[56] Henze, G. P. “An overview of optimal control for central cooling plants with ice thermal energy storage”. In: *Journal of Solar Energy Engineering, Transactions of the ASME* 125.3 (2003), pp. 302–309. DOI: 10.1115/1.1591801 (cit. on pp. 9, 10).

[57] Cui, B. et al. “Model-based optimal design of active cool thermal energy storage for maximal life-cycle cost saving from demand management in commercial buildings”. In: *Applied Energy* (2016). DOI: 10.1016/j.apenergy.2016.12.035 (cit. on pp. 9, 10).

[58] Tulus, V. et al. “Enhanced thermal energy supply via central solar heating plants with seasonal storage: A multi-objective optimization approach”. In: *Applied Energy* 181 (2016), pp. 549–561. DOI: 10.1016/j.apenergy.2016.08.037 (cit. on pp. 9, 10).

[59] IEA ECES Annex 30. *Applications of Thermal Energy Storage in the Energy Transition - Benchmarks and Developments: Public report (September 2018).* 2018 (cit. on pp. 9, 43).

[60] IEA ECES Annex 31. *Energy Storage with Energy Efficient Buildings and Districts: Optimization and Automation.* 2019 (cit. on pp. 9, 43).

[61] Del Pero, C. et al. “Energy storage key performance indicators for building application”. In: *Sustainable Cities and Society* 40 (2018), pp. 54–65. DOI: 10.1016/j.scs.2018.01.052 (cit. on pp. 9, 43).

[62] Cabeza, L. F. et al. “Evaluation of volume change in phase change materials during their phase transition”. In: *Journal of Energy Storage* 28 (2020), p. 101206. DOI: 10.1016/j.est.2020.101206 (cit. on p. 10).

[63] Ge, H. et al. “Low melting point liquid metal as a new class of phase change material: An emerging frontier in energy area”. In: *Renewable and Sustainable Energy Reviews* 21 (2013), pp. 331–346. DOI: 10.1016/j.rser.2013.01.008 (cit. on p. 10).

[64] Milián, Y. E. et al. “A review on encapsulation techniques for inorganic phase change materials and the influence on their thermophysical properties”. In: *Renewable and Sustainable Energy Reviews* 73 (2017), pp. 983–999. DOI: 10.1016/j.rser.2017.01.159 (cit. on p. 10).

[65] Lin, Y. et al. "Review on thermal conductivity enhancement, thermal properties and applications of phase change materials in thermal energy storage". In: *Renewable and Sustainable Energy Reviews* 82 (2018), pp. 2730–2742. DOI: 10.1016/J.RSER.2017.10.002 (cit. on p. 10).

[66] Nematpour Keshteli, A. and Sheikholeslami, M. "Nanoparticle enhanced PCM applications for intensification of thermal performance in building: A review". In: *Journal of Molecular Liquids* 274 (2019), pp. 516–533. DOI: 10.1016/J.MOLLIQ.2018.10.151 (cit. on p. 10).

[67] Zahir, M. H. et al. "Supercooling of phase-change materials and the techniques used to mitigate the phenomenon". In: *Applied Energy* 240 (2019), pp. 793–817. DOI: 10.1016/j.apenergy.2019.02.045 (cit. on pp. 10, 19, 33).

[68] Kenisarin, M. and Mahkamov, K. "Salt hydrates as latent heat storage materials: Thermophysical properties and costs". In: *Solar Energy Materials and Solar Cells* 145 (2016), pp. 255–286. DOI: 10.1016/j.solmat.2015.10.029 (cit. on p. 10).

[69] Fang, Y. et al. "An analytical technique for the optimal designs of tube-in-tank thermal energy storage systems using PCM". In: *International Journal of Heat and Mass Transfer* 128 (2019), pp. 849–859. DOI: 10.1016/j.ijheatmasstransfer.2018.08.138 (cit. on pp. 10, 62).

[70] ÅF Pöyry AB. *Innovation Project PCM Cold Storage: A Working Lab, Gothenburg (Internal Report)*. 2018 (cit. on pp. 11, 12).

[71] Jokiel, M. *Development and performance analysis of an object-oriented model for phase change material thermal storage: Project Report, SINTEF (2016)*. 2016 (cit. on pp. 12, 43).

[72] Alam, M. et al. "Energy saving performance assessment and lessons learned from the operation of an active phase change materials system in a multi-storey building in Melbourne". In: *Applied Energy* 238 (2019), pp. 1582–1595. DOI: 10.1016/j.apenergy.2019.01.116 (cit. on pp. 12, 43).

[73] Rubitherm GmbH. *https://www.rubitherm.eu/*. (Visited on 10/15/2019) (cit. on p. 13).

[74] BEKA Heiz- und Kühlmatten GmbH. *https://www.beka-klima.de/en/ice-energy-storage/: (Checked: 2019-10-15)*. (Visited on 10/15/2019) (cit. on pp. 13, 35).

[75] Rubitherm GmbH. *Safety Data Sheet SP6-14: Version from 2018-05-28* (cit. on p. 13).

[76] Tan, P. "On the Design Considerations for Thermal Energy Storage with Phase Change Materials: Material Characterization and Modelling". Licentiate Thesis. Chalmers University of Technology, 2018. URL: https://research.chalmers.se/publication/500367 (cit. on pp. 13, 37, 51, 62).

[77] Glicksman, M. E. *Principles of solidification: An introduction to modern casting and crystal growth concepts*. New York: Springer, 2011. ISBN: 1441973443 (cit. on p. 18).

[78] Mehling, H. et al. “The connection between the heat storage capability of PCM as a material property and their performance in real scale applications”. In: *Journal of Energy Storage* 13 (2017), pp. 35–39. DOI: 10.1016/j.est.2017.06.007 (cit. on p. 19).

[79] Lazaro, A. et al. “Intercomparative tests on phase change materials characterisation with differential scanning calorimeter”. In: *Applied Energy* 109 (2013), pp. 415–420. DOI: 10.1016/j.apenergy.2012.11.045 (cit. on pp. 19, 32).

[80] Barreneche, C. et al. “Study on differential scanning calorimetry analysis with two operation modes and organic and inorganic phase change material (PCM)”. In: *Thermochimica Acta* 553 (2013), pp. 23–26. DOI: 10.1016/j.tca.2012.11.027 (cit. on p. 19).

[81] Franquet, E. et al. “Inverse method for the identification of the enthalpy of phase change materials from calorimetry experiments”. In: *Thermochimica Acta* 546 (2012), pp. 61–80. DOI: 10.1016/j.tca.2012.07.015 (cit. on p. 19).

[82] Zhang, Y. and Jiang, Y. “A simple method, the T-history method, of determining the heat of fusion, specific heat and thermal conductivity of phase-change materials”. In: *Measurement Science and Technology* 10.3 (1999), p. 201 (cit. on pp. 19, 20).

[83] Hong, H. et al. “Accuracy improvement of T-history method for measuring heat of fusion of various materials”. In: *International Journal of Refrigeration* 27.4 (2004), pp. 360–366. DOI: 10.1016/j.ijrefrig.2003.12.006 (cit. on p. 19).

[84] Peck, J. H. et al. “A study of accurate latent heat measurement for a PCM with a low melting temperature using T-history method”. In: *International Journal of Refrigeration* 29.7 (2006), pp. 1225–1232. DOI: 10.1016/j.ijrefrig.2005.12.014 (cit. on p. 19).

[85] D’Avignon, K. and Kummert, M. “Assessment of T-History Method Variants to Obtain Enthalpy-Temperature Curves for PCMs With Significant Subcooling”. In: *Journal of Thermal Science and Engineering Applications* (2015). DOI: 10.1115/1.4031220 (cit. on p. 19).

[86] Mazo, J. et al. “A theoretical study on the accuracy of the T-history method for enthalpy-temperature curve measurement: analysis of the influence of thermal gradients inside T-history samples”. In: *Measurement Science and Technology* 26.12 (2015), p. 125001. DOI: 10.1088/0957-0233/26/12/125001 (cit. on pp. 19, 22).

[87] Lázaro, A. et al. “Verification of a T-history installation to measure enthalpy versus temperature curves of phase change materials”. In: *Measurement Science and Technology* 17.8 (2006), pp. 2168–2174. DOI: 10.1088/0957-0233/17/8/016 (cit. on pp. 19, 22).

[88] Hiebler, S. "Kalorimetrische Methoden zur Bestimmung der Enthalpie von Latentwärmespeichermaterialien während des Phasenübergangs: (in German)". PhD thesis. TUM, 2007 (cit. on pp. 19, 20, 22).

[89] Stanković, S. B. and Kyriacou, P. A. "Improved measurement technique for the characterization of organic and inorganic phase change materials using the T-history method". In: *Applied Energy* 109 (2013), pp. 433–440. DOI: 10.1016/j.apenergy.2013.01.079 (cit. on p. 19).

[90] Stankovic, S. "Investigation of advanced experimental and computational techniques for behavioural characterisation of phase change materials (pcms)". PhD thesis. City University London, 2014. URL: http://openaccess.city.ac.uk/3671/ (cit. on p. 19).

[91] Rathgeber, C. et al. "Measurement of enthalpy curves of phase change materials via DSC and T-History: When are both methods needed to estimate the behaviour of the bulk material in applications?" In: *Thermochimica Acta* 596.0 (2014), pp. 79–88. DOI: 10.1016/j.tca.2014.09.022 (cit. on p. 19).

[92] Brütting, M. et al. "Dynamic T-History method - A dynamic thermal resistance for the evaluation of the enthalpy-temperature curve of phase change materials". In: *Thermochimica Acta* 671 (2019), pp. 161–169. DOI: 10.1016/j.tca.2018.10.030 (cit. on pp. 19, 31, 32).

[93] Günther, E. et al. "Modeling of subcooling and solidification of phase change materials". In: *Modelling and Simulation in Materials Science and Engineering* 15.8 (2007), pp. 879–892. DOI: 10.1088/0965-0393/15/8/005 (cit. on p. 19).

[94] Safari, A. et al. "A review on supercooling of Phase Change Materials in thermal energy storage systems". In: *Renewable and Sustainable Energy Reviews* 70 (2017), pp. 905–919. DOI: 10.1016/j.rser.2016.11.272 (cit. on pp. 19, 33).

[95] Stefanescu, D. M. *Science and Engineering of Casting Solidification*. 3rd ed. 2015. SpringerLink : Bücher. Cham: Springer, 2015. ISBN: 3319156934 (cit. on p. 19).

[96] Englmair, G. et al. "Crystallization by local cooling of supercooled sodium acetate trihydrate composites for long-term heat storage". In: *Energy and Buildings* 180 (2018), pp. 159–171. DOI: 10.1016/j.enbuild.2018.09.035 (cit. on p. 19).

[97] Rathgeber, C. et al. "Analysis of supercooling of phase change materials with increased sample size - Comparison of measurements via DSC, T-History and at pilot plant scale". In: *Proceedings in Greenstock 2015 - 13th IEA ECES Conference*. 2015 (cit. on pp. 19, 20, 33).

[98] RAL Quality Association PCM e.V. *Phase Change Material - Quality Assurance: RAL-GZ 896*. 2018 (cit. on p. 20).

[99] Badenhorst, H. and Cabeza, L. F. "Critical analysis of the T-history method: A fundamental approach". In: *Thermochimica Acta* (2017). DOI: 10.1016/j.tca.2017.02.005 (cit. on p. 22).

[100] Eilers, P. H. C. “A perfect smoother”. In: *Analytical chemistry* 75.14 (2003), pp. 3631–3636. DOI: 10.1021/ac034173t (cit. on p. 27).

[101] Stickel, J. J. “Data smoothing and numerical differentiation by a regularization method”. In: *Computers & Chemical Engineering* 34.4 (2010), pp. 467–475. DOI: 10.1016/j.compchemeng.2009.10.007 (cit. on p. 27).

[102] Joint Committee for Guides in Metrology. *Evaluation of measurement data - Supplement 1 to the “Guide to the expression of uncertainty in measurement”: Propagation of distributions using a Monte Carlo method (JCGM 101:2008).* 2008 (cit. on p. 28).

[103] Gschwander, S. et al. *Development of a Test Standard for PCM and TCM Characterization: Part 1: Characterization of Phase Change Materials.* 2011 (cit. on p. 32).

[104] Mohamed, S. A. et al. “A review on current status and challenges of inorganic phase change materials for thermal energy storage systems”. In: *Renewable and Sustainable Energy Reviews* 70 (2017), pp. 1072–1089. DOI: 10.1016/j.rser.2016.12.012 (cit. on p. 33).

[105] Zondag, H. A. et al. “Performance analysis of industrial PCM heat storage lab prototype”. In: *Journal of Energy Storage* 18 (2018), pp. 402–413. DOI: 10.1016/j.est.2018.05.007 (cit. on pp. 33, 34).

[106] Xu, T. et al. “Thermal behavior of a sodium acetate trihydrate-based PCM: T-history and full-scale tests”. In: *Applied Energy* 261 (2020), p. 114432. DOI: 10.1016/j.apenergy.2019.114432 (cit. on pp. 33, 34).

[107] Englmair, G. et al. “Experimental investigation of a tank-in-tank heat storage unit utilizing stable supercooling of sodium acetate trihydrate”. In: *Applied Thermal Engineering* 167 (2020), p. 114709. DOI: 10.1016/j.applthermaleng.2019.114709 (cit. on p. 33).

[108] Kong, W. et al. “Experimental investigations on phase separation for different heights of sodium acetate water mixtures under different conditions”. In: *Applied Thermal Engineering* 148 (2019), pp. 796–805. DOI: 10.1016/j.applthermaleng.2018.10.017 (cit. on p. 34).

[109] Niyas, H. et al. “Performance investigation of a lab-scale latent heat storage prototype – Experimental results”. In: *Solar Energy* 155 (2017), pp. 971–984. DOI: 10.1016/j.solener.2017.07.044 (cit. on p. 34).

[110] Piette, M. A. “Analysis of a commercial ice-storage system: Design principles and measured performance”. In: *Energy and Buildings* 14.4 (1990), pp. 337–350. DOI: 10.1016/0378-7788(90)90096-2 (cit. on p. 43).

[111] Akbari, H. and Sezgen, O. “Performance evaluation of thermal energy storage systems”. In: *Energy and Buildings* 22.1 (1995), pp. 15–24. DOI: 10.1016/0378-7788(94)00898-T (cit. on p. 43).

[112] Nordell, B. and Skogsberg, K. "The Sundsvall Snow Storage - Six Years of Operation". In: *Thermal Energy Storage for Sustainable Energy Consumption.* Ed. by H. Paksoy. Springer, 2007, pp. 349–366. ISBN: 978-1-4020-5290-3 (cit. on p. 43).

[113] Voller, V. R. and Swaminathan, C. R. "General Source-Based Method for Solidification Phase Change". In: *Numerical Heat Transfer, Part B: Fundamentals* 19.2 (1991), pp. 175–189. DOI: 10.1080/10407799108944962 (cit. on p. 51).

[114] Rathgeber, C. et al. "IEA SHC Task 42 / ECES Annex 29 – A Simple Tool for the Economic Evaluation of Thermal Energy Storages". In: *Energy Procedia* 91 (2016), pp. 197–206. DOI: 10.1016/j.egypro.2016.06.203 (cit. on p. 55).

[115] Pinnau, S. and Breitkopf, C. "Determination of Thermal Energy Storage (TES) characteristics by Fourier analysis of heat load profiles". In: *Energy Conversion and Management* 101 (2015), pp. 343–351. DOI: 10.1016/j.enconman.2015.05.055 (cit. on p. 61).